MicroRNA-10 Regulates the Angiogenic Behavior of Zebrafish and Human Endothelial Cells by Promoting Vascular Endothelial Growth Factor Signaling

David Hassel, Paul Cheng, Mark P. White, Kathryn N. Ivey, Jens Kroll, Hellmut G. Augustin, Hugo A. Katus, Didier Y.R. Stainier and Deepak Srivastava

Circ Res. 2012;111:1421-1433; originally published online September 5, 2012;
doi: 10.1161/CIRCRESAHA.112.279711
Circulation Research is published by the American Heart Association, 7272 Greenville Avenue, Dallas, TX 75231

Print ISSN: 0009-7330. Online ISSN: 1524-4571

MicroRNA-10 Regulates the Angiogenic Behavior of Zebrafish and Human Endothelial Cells by Promoting Vascular Endothelial Growth Factor Signaling

David Hassel, Paul Cheng, Mark P. White, Kathryn N. Ivey, Jens Kroll, Hellmut G. Augustin, Hugo A. Katus, Didier Y.R. Stainier, Deepak Srivastava

Rationale: **Formation and remodeling of the vasculature during development and disease involve a highly conserved and precisely regulated network of attractants and repellants. Various signaling pathways control the behavior of endothelial cells, but their posttranscriptional dose titration by microRNAs is poorly understood.**

Objective: **To identify microRNAs that regulate angiogenesis.**

Methods and Results: **We show that the highly conserved microRNA family encoding miR-10 regulates the behavior of endothelial cells during angiogenesis by positively titrating proangiogenic signaling. Knockdown of miR-10 led to premature truncation of intersegmental vessel growth in the trunk of zebrafish larvae, whereas overexpression of miR-10 promoted angiogenic behavior in zebrafish and cultured human umbilical venous endothelial cells. We found that miR-10 functions, in part, by directly regulating the level of fms-related tyrosine kinase 1 (FLT1), a cell-surface protein that sequesters vascular endothelial growth factor, and its soluble splice variant sFLT1. The increase in FLT1/sFLT1 protein levels upon miR-10 knockdown in zebrafish and in human umbilical venous endothelial cells inhibited the angiogenic behavior of endothelial cells largely by antagonizing vascular endothelial growth factor receptor 2 signaling.**

Conclusions: **Our study provides insights into how FLT1 and vascular endothelial growth factor receptor 2 signaling is titrated in a microRNA-mediated manner and establishes miR-10 as a potential new target for the selective modulation of angiogenesis. (*Circ Res*. 2012;111:1421-1433.)**

Key Words: angiogenesis ■ developmental biology ■ fms-related tyrosine kinase 1 ■ microRNA ■ vascular endothelial growth factor

The circulatory system consists of a highly organized network of blood vessels that distributes nutrients, gases, and hormones throughout the body. Its formation is highly conserved and requires the coordination of 2 distinct cellular processes. During embryonic development, proliferating endothelial precursor cells migrate and differentiate in response to regional signaling cues to form a primitive lumenized vascular plexus, a process known as vasculogenesis. Through angiogenesis, this plexus is remodeled and extended by new blood vessel growth and addition of smooth muscle cells and pericytes.

In addition to regulating various physiological processes, such as development, organ growth, and immune and injury responses, the vasculature is involved in several pathophysiological conditions, including diabetic retinopathy and tumor growth.[1] Strategies targeting angiogenesis have proven to be valuable therapeutic approaches in preventing tumor progression.[2]

In This Issue, see p 1387
Editorial, see p 1388

The establishment and remodeling of the vascular system depends on a precisely orchestrated interplay of attractants and repellants in which several secreted signaling molecules, including vascular endothelial growth factor (VEGF), fibroblast growth factor, and platelet-derived growth factor, and their

Original received December 6, 2011; revision received August 31, 2012; accepted September 30, 2012. In August 2012, the average time from submission to first decision for all original research papers submitted to *Circulation Research* was 11.48 days.

From the Gladstone Institute of Cardiovascular Disease, San Francisco, CA (D.H., P.C., M.P.W.,K.N.I., D.S.); Roddenberry Center for Stem Cell Biology and Medicine at Gladstone, San Francisco, CA (D.H., P.C., M.P.W., K.N.I., D.S.); Department of Pediatrics, University of California, San Francisco, San Francisco, CA (D.H., P.C., M.P.W., K.N.I., D.S.); Department of Biochemistry and Biophysics, University of California, San Francisco, San Francisco, CA (D.H., P.C., M.P.W., D.Y.R.S., D.S.), Department of Vascular Biology and Tumor Angiogenesis, Center for Biomedicine and Medical Technology Mannheim, Mannheim, Germany (J.K., H.G.A.); Division of Vascular Oncology and Metastasis, German Cancer Research Center (DKFZ-ZMBH Alliance), Heidelberg, Germany (J.K., H.G.A.); Department of Medicine III, Cardiology, University of Heidelberg, Heidelberg, Germany (D.H., H.A.K.); and Department of Developmental Genetics, Max Planck Institute for Heart and Lung Research, Bad Nauheim, Germany (D.Y.R.S.).

The online-only Data Supplement is available with this article at http://circres.ahajournals.org/lookup/suppl/doi:10.1161/CIRCRESAHA.112.279711/-/DC1.

Correspondence to Deepak Srivastava, Gladstone Institute of Cardiovascular Disease, and University of California, San Francisco, 1650 Owens Street, San Francisco, CA, 94158 (e-mail dsrivastava@gladstone.ucsf.edu); or David Hassel, Department of Medicine III, Cardiology, University of Heidelberg, Im Neuenheimer Feld 410, 69120 Heidelberg, Germany (e-mail david.hassel@med.uni-heidelberg.de).

Circulation Research **is available at http://circres.ahajournals.org** **DOI: 10.1161/CIRCRESAHA.112.279711**

Non-standard Abbreviations and Acronyms	
hpf	hours postfertilization
HUVEC	human umbilical venous endothelial cell
ISV	intersegmental vessel
miRNA	microRNA
NLS	nuclear localization signal

corresponding receptors transduce downstream signaling events that subsequently result in the modulation of endothelial cell behavior. The most potent of these angiogenic signaling factors, VEGF, functions by binding to 1 of 3 cognate receptor tyrosine kinases (VEGF receptor [VEGFR] 1–3).[3,4] Gene-targeting approaches in mice demonstrated a particularly important role for VEGFR2 (also known as kinase insert domain receptor [KDR]) in VEGF-mediated signaling, because VEGFR2-null mice die at embryonic day 8.5 to 9 because of defective blood-island formation and the near absence of vasculature.[5] Stimulation of KDR with VEGF results in KDR autophosphorylation and activation of several well-studied signal transduction pathways.

In contrast, the role of VEGFR1 (or fms-related tyrosine kinase 1 [FLT1]) during vessel formation remains controversial. In mice, depletion of FLT1 results in early embryonic lethality at embryonic day 8.5 to 9 because of increased hemangioblast commitment and disorganized blood vessel development as a result of endothelial cell overgrowth and excessive KDR activation. This suggests that FLT1 and its soluble splice variant sFLT1 (containing the extracellular VEGF-binding domain only) negatively regulate KDR signaling.[6,7] In support of this concept, KDR phosphorylation levels are increased in embryonic stem cells (ESCs) lacking FLT1.[8] Despite a ≥10-fold higher affinity for VEGF than KDR, the level of FLT1 phosphorylation after VEGF exposure is extremely low.[9] Mice lacking the kinase domain of FLT1 have normal vasculature development, supporting the idea that FLT1 fine-tunes KDR signaling by sequestering VEGF and preventing it from binding to KDR.[9,10] Although KDR and FLT1 seem to be important for vascular endothelial cell development, various genetic studies implicated a particularly important role for VEGFR3 (FLT-4) in establishing and maintaining lymphatic endothelial cells.[11,12] In vascular endothelial cells, VEGFR3/FLT-4 functions mainly in arterial/venous endothelial cell determination during intersegmental vessel sprouting through its ligand VEGF-C.[13,14]

In light of the complexity among angiogenic and antiangiogenic stimuli, careful balancing of signals that control endothelial cell behavior is essential for the establishment, maintenance, and remodeling of the vasculature.[15] In addition to known proteins that regulate downstream kinase activation cascades, the posttranscriptional titration of key angiogenic signaling nodes by microRNAs (miRNAs) has gathered particular interest.[16] miRNAs are small, single-stranded, endogenous noncoding RNAs averaging 22 nucleotides in length. miRNAs bind to target mRNAs based on sequence complementarity, as well as accessibility of the potential target site, and negatively regulate gene expression by either translational inhibition or destabilization of target mRNAs.[17] Several miRNAs regulate angiogenic signaling, including miR-126, members of the miR-17 to miR-92 cluster and miR-21.[18–21]

miR-10 function is dysregulated in various cancers, in which it was implicated in mediating tumor invasion and metastasis by altering the levels of its target, homeobox D10 (HOXD10).[22] However, little is known about its function in endothelial cells. Fang et al[23] recently demonstrated an involvement for miR-10 in regulation of the proinflammatory response in athero-susceptible endothelium by directly targeting key regulators of nuclear factor-κB activation. Additionally, Shen et al[24] demonstrated a role for miR-10b in regulating angiogenesis specifically in response to thrombin through down regulation of HOXD10.[24] Here, we describe a novel role for miR-10 in modulating the angiogenic behavior of endothelial cells during development, in part, through direct regulation of FLT1 and its soluble splice isoform sFLT1.

Methods

Care and breeding of zebrafish (*Danio rerio*) was performed essentially as described.[25] The *Tg(kdrl:EGFP)s843* and *Tg(kdrl:nlsEGFPzf*^{109}*), Tg(kdrl:HsHRAS-mCherrys*^{896}*)*[26,27] strains were used. For immunofluorescence analysis in zebrafish, we used anti-MF20 (Developmental Studies Hybridoma Bank; 1:5) and anti-znp1 (Developmental Studies Hybridoma Bank; 1:100) antibodies.

Human umbilical vein endothelial cells (HUVECs) and recommended medium were purchased from ScienCell and cultured according to manufacturer's recommendations.

Undifferentiated mouse ESCs were propagated on gelatin-coated cell culture plastic (Nunc) in Glasgow minimum essential medium supplemented with 10% fetal bovine serum, 0.1 mmol/L nonessential amino acids, 2 mmol/L GlutaMAX, 0.1 mmol/L sodium pyruvate (Invitogen), 0.1 mmol/L 2-mercaptoethanol (Sigma-Aldrich), and 1500 U/mL leukemia inhibitory factor (LIF; Millipore). ESC were passaged every 2 to 3 days with TrypLE Express (Invitrogen) with daily medium changes. ESCs were dissociated to single cells and differentiated as embryoid bodies in ultra-low attachment plates (Corning) in Glasgow minimum essential medium supplemented with penicillin/streptomycin, 2 mmol/L GlutaMAX, 0.1 mmol/L nonessential amino acids (Sigma-Aldrich), and 20% fetal bovine serum at a final concentration of 100 000 cells/mL.

The following antibodies were used: anti-Flk1 (BD Pharmigen; 560680), anti-VE-cadherin (Ebio-17–1441), anti-FLT1 (Abcam; 1:500), anti-KDR (Cell Signaling; 1:2000), anti-phospho-KDR (Cell Signaling; 1:1000), anti-GAPDH (Santa Cruz; 1:2000), and anti-HOXD10 (Santa Cruz; 1:200), anti phosphohistone H3 (Cell Signaling; 1:200), and andanti–Annexin V (Abcam; 1:200). For phospho-KDR Western blots, HUVEC were serum-starved overnight and then treated with 2 or 10 ng/mL human recombinant VEGF (BD Biosciences) as indicated for 10 min.

For all the other experimental details, see the Online Data Supplement.

Results

miR-10 Expression Is Induced After Mesoderm Specification in ESCs and Is Enriched in KDR$^+$ Cells

The miR-10a/10b isoforms are encoded in a highly conserved location within the developmental regulator cluster of homeobox (HOX) genes, a feature shared only by miR-196 and miR-615 (Online Figure I).[28,29] To determine when miR-10 expression is induced during early development, we assayed miR-10a and miR-10b expression, along with several marker genes, by quantitative reverse-transcriptase polymerase chain reaction, using mRNA derived from embryoid bodies at progressive stages of differentiation from mouse ESCs (Figure 1A and 1B). *Brachyury*, a marker of early mesoderm, was dramatically induced at day 4 of differentiation, as was *Sox17*, a marker of endoderm (Figure 1A). Expression of miR-10a and miR-10b

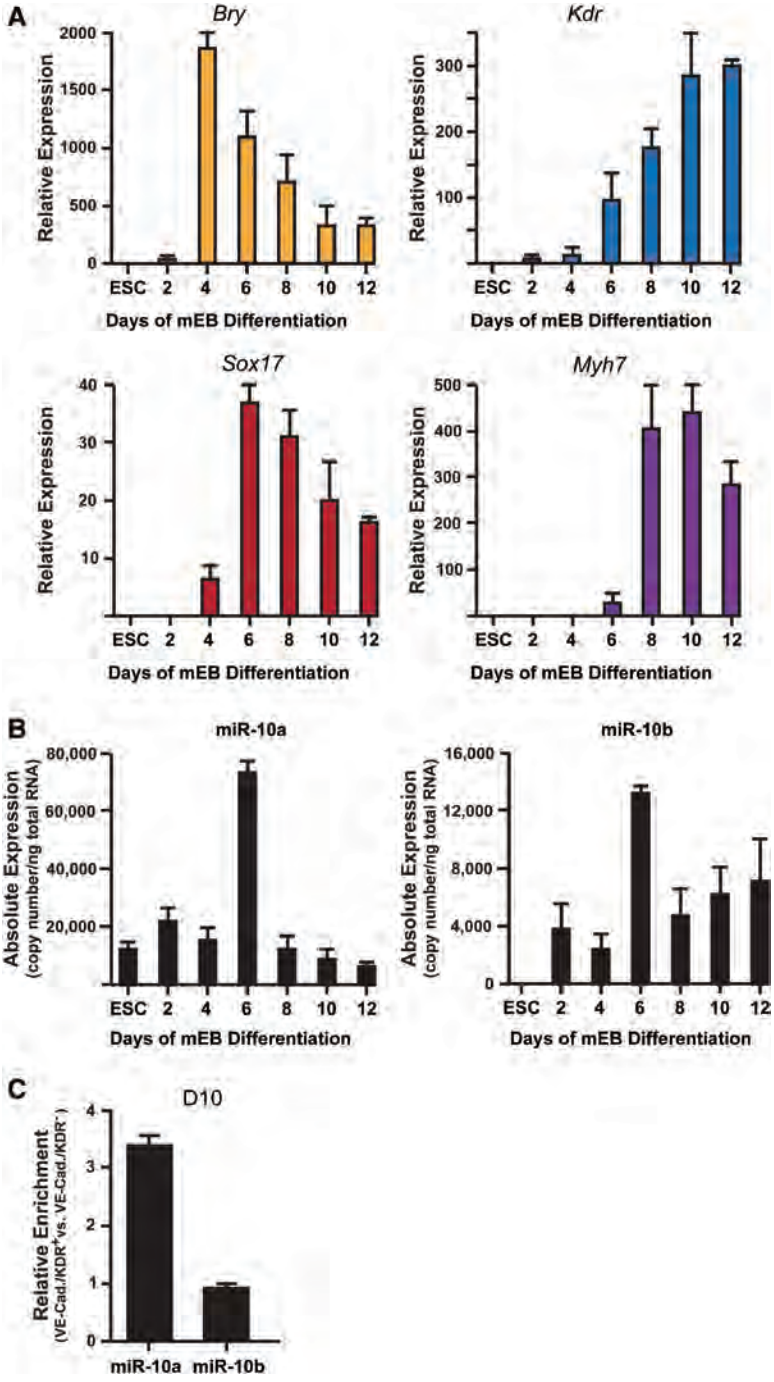

Figure 1. MicroRNA (miR)-10 is expressed in endothelial cells. Quantitative reverse-transcriptase polymerase chain reaction studies of (**A**) marker gene expression during mouse embryonic stem cells (mESC) differentiation into embryoid bodies (EBs); (**B**) absolute expression levels of miR-10a and miR-10b in differentiating EBs; and (**C**) relative levels of miR-10a and miR-10b in VE-cadherin$^+$/KDR$^+$ vs VE-cadherin$^-$/KDR$^-$ cells in day 10 EBs. Values are displayed as mean±SD, **P*<0.05; n=4. Bry indicates Brachyury; kdr, kinase insert domain receptor; mEB, mouse embryoid bodies.

was significantly upregulated after mesoderm and endoderm induction at day 6 (Figure 1B). Interestingly, *KDR/VEGFR2* expression was similarly induced at day 6 and further increased until day 10, suggesting that miR-10 might get induced in differentiating KDR-positive populations. During mouse ESC differentiation, miR-10a was expressed more abundantly than miR-10b (Figure 1B). The cardiomyocyte marker *Myh7* was robustly detected at D8 (Figure 1A).

We next tested whether miR-10 might be expressed and enriched in endothelial cells and found that miR-10a but not miR-10b was almost 3.4-fold enriched in KDR/VE-cadherin–positive endothelial cells compared with KDR/VE-cadherin-negative nonendothelial cells (Figure 1C).

miR-10 Regulates Angiogenesis In Vivo

Zebrafish express up to 4 miR-10 isoforms (miR-10a-d) encoded in 5 independent transcripts (Figure 2A). By quantitative reverse-transcriptase polymerase chain reaction, we found that expression of all 4 isoforms was induced at 14 hours post-fertilization (hpf) and peaked at 20 hpf (Figure 2B). By 24 and 48 hpf, miR-10a and miR-10b levels had decreased, whereas the expression levels of miR-10c and miR-10d were similar to those found at 14 hpf (Figure 2B).

To investigate loss-of-function effects during development, we injected 2 unique morpholino (MO)-modified oligonucleotide mixtures (MO-miR-10 and MO-miR-10*) into

1-cell-stage zebrafish embryos (Figure 2C). MO-miR-10 consists of 2 MOs that block the processing of pri-miR-10a and pri-miR-10b-1, resulting in profoundly reduced levels of mature miR-10a and miR-10b and, because of high homology, miR-10c and miR-10d (Figure 2A and 2D). MO-miR-10* consists of 4 MOs that target pre-miR-10 star isoforms (Figure 2A), which affect the processing of the mature miRNA and its corresponding star isoform.[30] Injecting MO-miR-10* decreased mature miR-10 levels similar to MO-miR-10, demonstrating the efficacy of both MOs (Figure 2D). Importantly, the level of zebrafish *hoxb4a*, where miR-10c resides intronically, was not appreciably altered by miR-10 MOs (Figure 2D).[31] Reduction of miR-10 levels by MO-miR-10 or MO-miR-10* led to identical angiogenic phenotypes (Online Figure II). Because injection of MO-miR-10 was slightly more efficient in decreasing mature miR-10 levels and led to a more robust phenotype, all subsequent experiments were performed with this MO mixture.

At 72 hpf, MO-miR-10–injected and control-injected embryos had no differences in gross morphology (Figure 2C, top row). However, examination of transgenic zebrafish expressing green fluorescent protein under the control of an endothelial-specific promoter, which marks the vasculature [*Tg(kdrl:EGFP)*^{s843}], revealed that tail blood vessel formation was strongly affected by MO-miR-10 injection (Figure 2C).

The intersegmental vessels (ISV) in the zebrafish tail first sprout from the dorsal aorta and subsequently grow dorsally to form the dorsal longitudinal anastomotic vessel. By 72 hpf, the ISVs in control embryos are aligned well and fully developed (Figure 2C, bottom panel).[32] In contrast, in miR-10-deficient embryos, ≈6% of ISVs completely failed to sprout, whereas 50% of the sprouting ISVs stopped at the horizontal myoseptum, instead forming an ectopic longitudinal anastomotic vessel centered along the midline (Figure 2C and 2E). Furthermore, although some ISVs in MO-miR-10–injected embryos showed proper growth, 80% of all scored miR-10-deficient ISVs displayed defective formation of the dorsal longitudinal anastomotic vessel (Figure 2C and 2E).

miR-10 also regulates the expression of several Hox genes.[22,31,33] Hox gene function is essential for correct anterior–posterior patterning and normal somite morphogenesis during embryogenesis. Because dysmorphic or mispatterned somites can cause vascular defects, we evaluated whether miR-10-deficient embryos had development of normal somites.[34,35] Immunolabeling of myosins in the somites (Online Figure IIA) and synaptotagmin-2 in motorneurons (Online Figure IIB) revealed normal somite boundaries and typical v-shape appearance in miR-10-deficient embryos.[36]

Knockdown of miR-10 Affects Angiogenic Behavior of HUVECs In Vitro

The high conservation of miR-10 between zebrafish and humans enabled us to use a single zebrafish MO to block processing of pre-miR-10 into mature miR-10 in HUVECs (Figure 2A and Online Figure I). Electroporation of this morpholino significantly decreased both mature miR-10a and miR-10b levels (Figure 3A). Importantly, mRNA levels of *Hoxd3*, where miR-10b is intronically encoded and which spans the *Hoxd4* locus, were unaffected (Figure 3A).

VEGF exposure significantly increased cell number in serum-starved control but not in miR-10-deficient HUVECs (Figure 3B), whereas transfection of a miR-10 mimic enhanced cell proliferation in response to VEGF compared with mock-transfected cells. Immunostaining for the cell death marker Annexin V confirmed that miR-10-deficient HUVECs did not display increased cell death, suggesting that miR-10 affects VEGF-mediated cell proliferation (Figure 3C). To assess how miR-10 depletion affects the angiogenic potential of HUVECs, we used a matrigel capillary tube formation assay to assess sprouting activity and capillary network complexity. miR-10 deficiency in HUVECs resulted in significantly shorter tube length and fewer branching points after 24 hours than in control cells, indicating overall reduced angiogenic potential (Figure 3D). Interestingly, overexpression of miR-10 led to similar tube lengths as observed in control but significantly more sprouting and branching activity (Figure 3D). Furthermore, lentiviral-mediated knockdown of miR-10 decreased angiogenic potential in a HUVEC 3-dimensional spheroid-based sprouting assay (Figures 4A and Online Figure VIIA). We next examined migratory potential after VEGF exposure using the scratch (wound closure) assay. In control-transfected confluent HUVEC cultures, cells quickly began to migrate into the cell-cleared area after the scratch, and the wound closed 28±10% by 8 hours and 70±10% after 24 hours. In contrast, cell migration into the wound area of miR-10-deficient HUVECs was severely reduced, with only 17±2% (P<0.05) at 8 hours and 30±7% closure by 24 hours (P<0.0002) (Figure 3E). Conversely, overexpression resulted in a significantly increased migratory behavior, with 30±11% and 84±10% wound closure at 8 and 24 hours, respectively (Figure 3E). Furthermore, kinetic measurements of cell attachment revealed significantly lower adhesion of MO-miR-10-deficient HUVECs than controls (Online Figure IV).

To evaluate whether miR-10-deficient HUVECs also display less angiogenic potential in situ, we engrafted control and miR-10 knockdown cells subcutaneously into mice using a matrigel xenografting assay.[37,38] The reduction of miR-10 in the HUVEC xenograft resulted in decreased mean vessel density compared with control-transduced cells (P<0.05) (Figure 4B).

miR-10 Deficiency Affects Endothelial Cell Behavior In Vivo

Because miR-10 depletion significantly affected human endothelial cell behavior, we evaluated its effects in vivo in double-transgenic zebrafish that expressed nuclear-localizing green fluorescent protein and cytoplasmic mCherry in all endothelial cells of the vasculature [*Tg(kdrl:nlsEGFPzf*^{109}*; Tg(kdrl:HsHRAS-mCherrys*^{896}*)*]. In scrambled control-MO–injected embryos, ISV cells emerged from the dorsal aorta at approximately 20 hpf and migrated dorsally. At 24 hpf, the majority of control ISVs consisted of 2 (49.96±12%) or 3 (34.16±7%) endothelial cells evenly distributed over the length of the ISV from the dorsal aorta to approximately the level of the horizontal myoseptum (Figure 5A, 5B). Thereafter, ISVs continued to migrate dorsally until they reached coalesced to

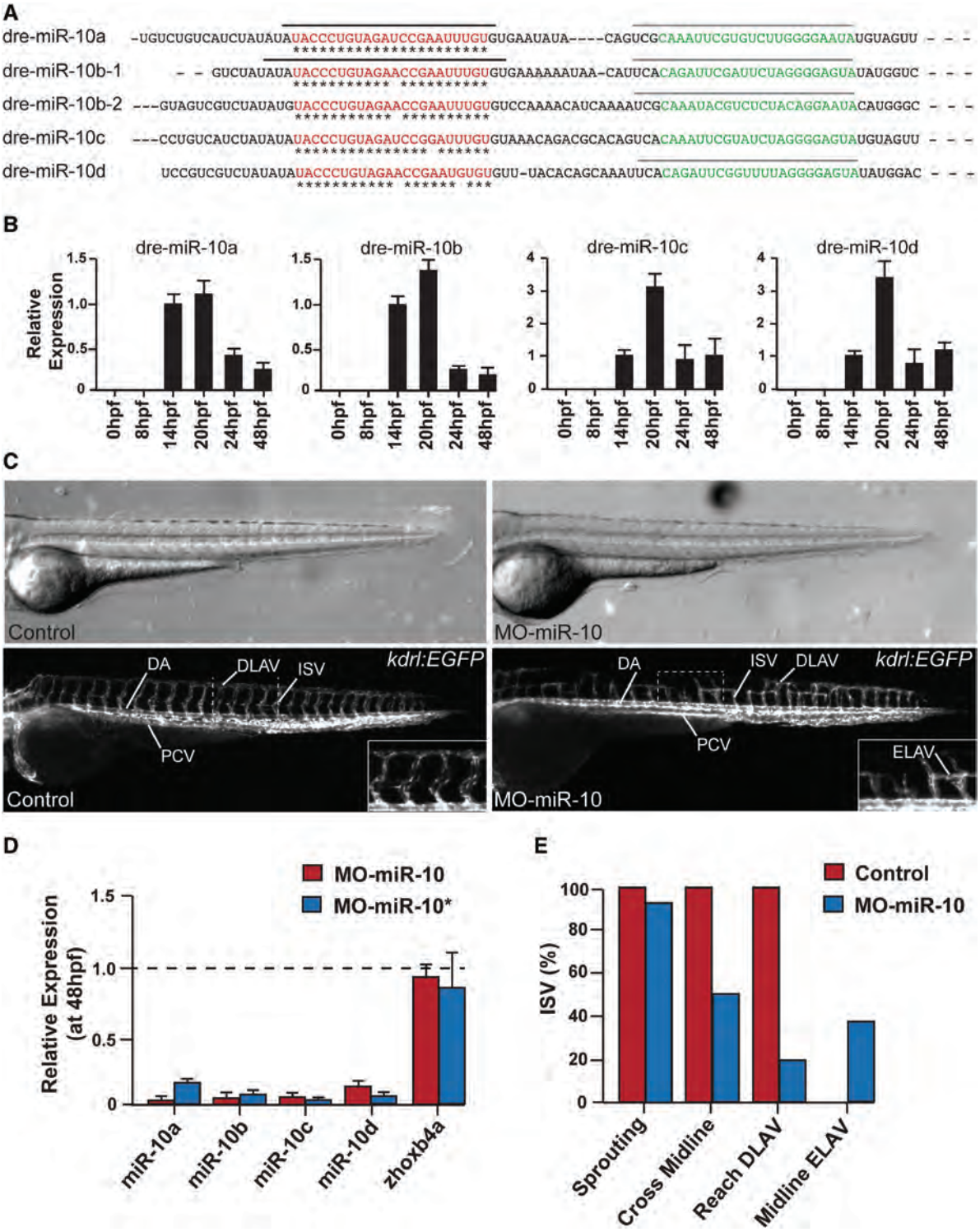

Figure 2. Knockdown of microRNA (miR)-10 leads to defects in vascular development in zebrafish. A, Schematic representation of morpholino (MO) location (black bars for MO-miR-10; grey bars for MO-miR-10*) within the precursor used to target miR-10 processing into mature miR-10 (red letters) and mature miR-10* (green) in zebrafish. **B**, Expression of the different miR-10 isoforms during zebrafish development assayed by quantitative reverse-transcriptase polymerase chain reaction (qRT-PCR) relative to 14 hpf expression. **C**, Lateral brightfield (top) and fluorescent (bottom) images of *Tg(kdrl:EGFP)*^{s843} control-injected and MO-miR-10–injected embryos at 72 hours postfertilization (hpf). Brightfield images (top) revealed no overall morphological changes on miR-10 knockdown. Fluorescent images (bottom) showed severe angiogenesis defects. High magnification is shown in insets. **D**, Relative expression of genes assessed by qRT-PCR in MO-miR-10 or MO-miR-10*–injected embryos at 48 hpf compared with age-matched control-injected embryos. **E**, Quantification of individual intersegmental vessel (ISV) phenotypes (n=200, >25 embryos) based on initiation of vessel sprouting from the dorsal aorta (sprouting), vessel crossing the ventral–dorsal midline (cross midline), reaching the dorsal longitudinal anastomotic vessel ([DLAV]; reach DLAV), and formation of premature ectopic longitudinal anastomotic vessel (ELAV) in the ventral-dorsal midline (midline ELAV). DA, dorsal aorta; PCV, posterior cardinal vein.

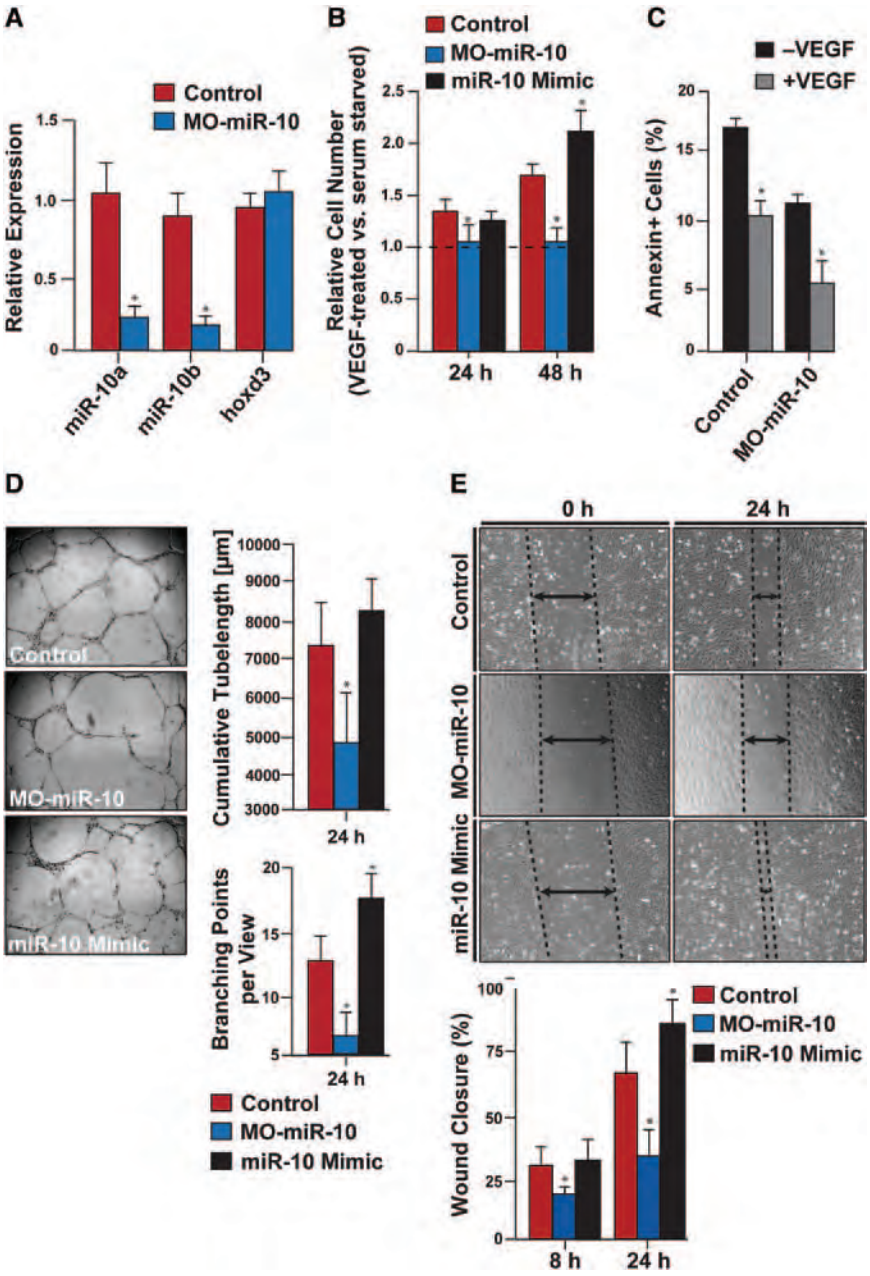

Figure 3. MicroRNA (miR)-10 affects human endothelial cell behavior in vitro. **A**, Relative levels of miR-10a, miR-10b, and hoxd3 by quantitative polymerase chain reaction 48 hours after electroporation of morpholino (MO)-miR-10 compared with control-transfected human umbilical venous endothelial cells (HUVECs). **B**, Changes in cell number in response to vascular endothelial growth factor (VEGF; 10 ng/mL) assayed in control, MO-miR-10, or miR-10 mimic–transfected HUVECs (*P<0.05 compared with controls). **C**, Annexin V staining of control-transfected or MO-miR-10–transfected HUVECs with or without VEGF. **D**, Representative images and quantitative analysis of capillary tube formation assay of HUVECs (×20 magnification) (*P<0.05 compared with controls; n=3). **E**, Endothelial cell migration of control-transfected, MO-miR-10–transfected, or miR-10 mimic–transfected HUVECs in response to VEGF (10 ng/mL) determined using a scratch assay. Dashed lines indicate width of gap. Representative images at time of generating scratch (0 hours) and 24 hours after are shown. Percent wound closure at 8 and 24 hours after scratch is shown. Values in graphs are shown as mean±SD. *P<0.05; n=5.

form the dorsal longitudinal anastomotic vessel at ≈30 hpf. At 48 hpf, the majority of ISVs consisted of 4 (53.2±10%) or 5 (31.89±11%) endothelial cells evenly distributed between the dorsal aorta and the dorsal longitudinal anastomotic vessel (Figure 5A and 5C). In 24 hpf miR-10-deficient embryos, most ISVs reached the horizontal myoseptum, although some ISVs failed to sprout (Figure 5A). However, most had significantly fewer cells or ISV (Figure 5B). At 48 hpf, most ISVs in MO-miR-10–injected embryos grew only halfway, halting at the horizontal myoseptum, with the majority of ISVs consisting of 2 endothelial cells (48.9±11%) (Figure 5A and 5C). Notably, endothelial cells aggregated within ISVs and were seemingly unable to separate during dorsal migration, suggesting defective migration (Figure 5A).

To determine whether miR-10 overexpression could promote angiogenic behavior in vivo, we injected miR-10 mimic into *Tg(kdrl:EGFP)s843* transgenic fish. miR-10 overexpression had no obvious morphological defects (Figure 5D), and overall angiogenesis appeared normal. However, by 48 hpf, zebrafish expressing excess miR-10 had development of pericardial edema accompanied by blood congestion at the inflow tract, indicative of cardiac dysfunction (Figure 5D). Interestingly, *Tg(kdrl:nlsEGFPzf*^{109} and *Tg(kdrl:HsHRAS-mCherrys*^{896} embryos overexpressing miR-10 revealed a significant increase in endothelial cells or ISV at 50 hpf (Figure 5E and 5F), indicating that miR-10-overexpressing endothelial cells have enhanced angiogenic potential in vivo.

miR-10 Directly Modulates FLT1 Levels Posttranscriptionally

To understand the molecular mechanism by which miR-10 modulates endothelial cell behavior, we searched for direct

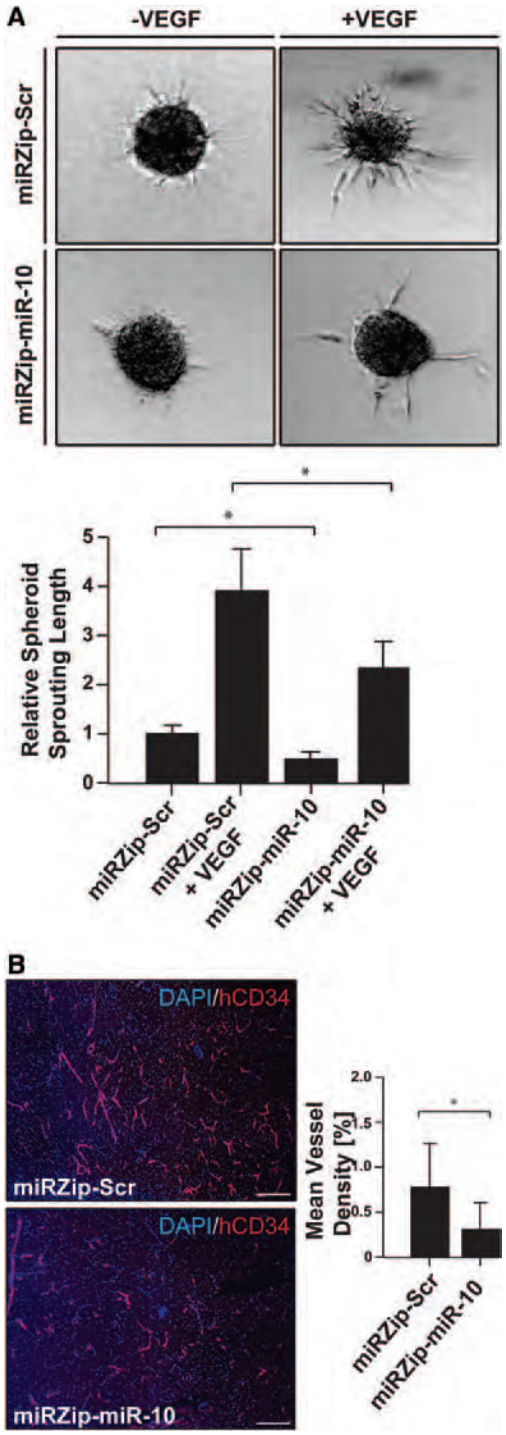

Figure 4. Reduced microRNA (miR)-10 function interferes with angiogenesis. A, Representative images of human umbilical venous endothelial cells (HUVECs) infected with a scrambled control lentivirus (miRZip-Scr) or a lentiviral construct designed to specifically block miR-10 for 24 hours, miRZip-miR-10, followed by a spheroid assay. Quantification of relative cumulative sprout length with or without is displayed (n=5). **B**, Vessel network formation of miRZip-Scr-transduced or miRZip-miR-10–transduced HUVECs in a Matrigel xenografting assay. Sections (0.5 μm) were stained for human CD34 (red) and costained with 4,6-diamidino-2-phenylindole (DAPI; blue) and whole matrigel plugs were analyzed for mean vessel density (*P<0.05; n=30 from 5 independent mouse experiments). Representative pictures from regions of high vessel density selected from whole matrigel plugs are shown. Scale bar, 200 μmol/L.

miR-10 targets using microRNA prediction programs, including an algorithm developed in our laboratory that integrates sequence complementarity and mRNA target site accessibility (K. Ivey, PhD, D. Srivastava, MD, unpublished data). We cloned the 3′ untranslated region (UTR) of putative targets containing the possible miR-10-binding site into the 3′ UTR of a luciferase construct and tested the ability of miR-10 to repress luciferase expression in COS-7 cells. We chose the 3′ UTR of the validated miR-10 target HOXD10 as a positive control and tested the 3′ UTRs of FLT1, its soluble splice variant sFLT1, and sprouty 4 based on binding sites and their known function in regulating endothelial cell biology.[21,39,40] miR-10 significantly repressed the expression of luciferase constructs containing the 3′ UTR of HOXD10, FLT1, and sFLT1, but not sprouty homolog 4 (Figure 6A and 6B and Online Figure VI). Importantly, mutating the potential binding site for miR-10 in the 3′ UTR of HOXD10, FLT1, and sFLT1 abolished miR-10-dependent repression of luciferase activity.

By quantitative reverse-transcriptase polymerase chain reaction, we found that mRNA levels derived from miR-10-deficient HUVECs were unchanged; however, *FLT1* levels from MO-miR-10–injected zebrafish were significantly upregulated, suggesting differential effects of miR-10 on *FLT1* mRNA in humans and zebrafish (Figure 6C). Strikingly, FLT1 protein levels were dramatically upregulated in miR-10-deficient cells compared with control HUVECs (Figure 6D). Additionally, by ELISA we found a 3.4±0.58-fold (P<0.05) increase in sFLT1 protein levels in the supernatant of MO-miR-10–transfected HUVECs compared with control-transfected cells (Figure 6E). These results clearly show that miR-10 directly targets the 3′ UTR of FLT1 and sFLT1, and thereby titrates the level of FLT1/sFLT1 protein.

Increased FLT1 Levels in miR-10 Deficiency Antagonize KDR-Dependent Signaling

Although much is known about VEGF receptor 2 (KDR) signaling and function in endothelial cells, comparatively little is known about the function of FLT1; however, it is thought to function, in part, by preventing VEGF binding to KDR.[6,41] Since FLT1 has a significantly higher affinity for VEGF than KDR, we hypothesized that increased levels of FLT1 upon miR-10 deficiency would compete for VEGF binding under low VEGF conditions, putatively resulting in decreased VEGF-KDR binding. We measured VEGF-mediated autophosphorylation of KDR in control or MO-miR-10–transfected HUVECs cultured with low levels of VEGF (2 ng/mL) and found that knockdown of miR-10 caused a heterogeneous but significant decrease in KDR phosphorylation (Figure 6F). Interestingly, higher doses of VEGF (10 ng/mL) resulted in similar phosphorylation of KDR in miR-10-deficient HUVECs and controls, yet phenotypic defects persisted (Figures 3B–3E and 6F), suggesting that signaling downstream of FLT1 also may contribute to the observed anti-angiogenic effect.[8,39,42,43]

To test whether reduced KDR function might cause angiogenesis defects similar to miR-10 deficiency, we treated 20 hpf embryos in which trunk vessels already had developed, but ISVs had not started to sprout, with low doses of the

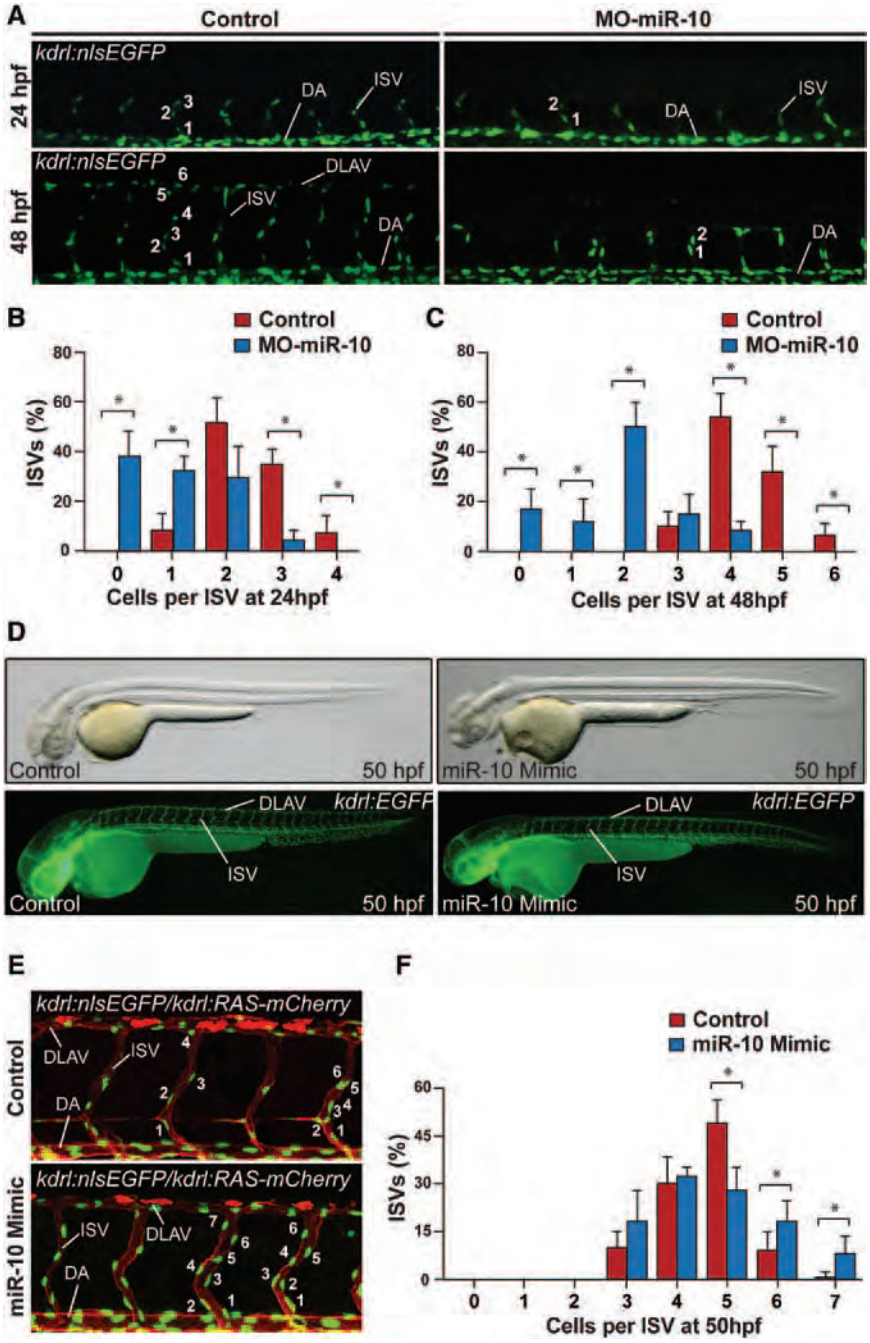

Figure 5. MicroRNA (miR)-10 regulates endothelial cell division and migration in vivo. A, Proper addition of endothelial cells and migrational behavior of individual cells during dorsal migration of intersegmental vessels (ISVs) in control and morpholino (MO)-miR-10–injected embryos were assayed in *Tg(kdrl:nlsEGFPzf*^{109}*; kdrl:HsHRAS-mCherrys*^{896}) transgenic zebrafish. Images are representative lateral views of 24 hours postfertilization (hpf) or 48 hpf control-injected or MO-miR-10–injected embryos; numbers indicate endothelial cells in ISVs. **B**, Percent of ISVs with indicated cells/ISV in control-injected or MO-miR-10–injected embryos at 24 hpf. **C**, Percent of cells/ISV in control-injected or MO-miR-10–injected embryos at 48 hpf (n≥200 individual ISVs from >25 randomly selected larvae per condition). **D**, Lateral views of *Tg(kdrl:EGFP)s*^{843}control-injected or miR-10-mimic–injected embryos at 50 hpf. Besides pericardial edema(*), brightfield images (top) revealed no overall morphological changes on miR-10 knockdown. Fluorescent images (bottom) show normal overall angiogenesis upon miR-10 overexpression compared with control larvae. **E**, Representative confocal images of *Tg(kdrl:nlsEGFPzf*^{109}*; kdrl:HsHRAS-mCherrys*^{896}) transgenic control-injected and miR-10-mimic–injected zebrafish larvae at 50 hpf. **F**, Percent of cells/ISV in control-injected or miR-10-mimic–injected embryos at 50 hpf. DA, dorsal aorta; DLAV, dorsal longitudinal anastomotic vessel; ISV, intersegmental vessel; EGFP, enhanced green fluorescent protein.

VEGFR2-specific inhibitor SU5416.[44] At 30 hpf, inhibitor-treated embryos displayed blunted growth of ISVs stalled at the midline and significantly fewer endothelial cells per ISV (Figure 7A). Hence, pharmacological inhibition of KDR activity results in an angiogenic phenotype closely resembling miR-10 deficiency. To determine whether increased FLT1 and sFLT1 levels could induce angiogenesis defects similar to decreased miR-10 in vivo, we injected full-length FLT1 mRNA in zebrafish. This resulted in ISV profiles similar to KDR inhibition, consisting of predominantly 2 endothelial cells (Figure 7A). Increasing sFLT1 resulted in a more dramatic decrease in angiogenesis with significantly more ISVs consisting of only 0 to 1 cell per ISV, suggesting a more potent negative regulatory potential of sFLT1 on proangiogenic KDR signaling compared with full-length FLT1 (Figure 7A). Thus, increased expression of FLT1 mimics many of the angiogenic defects of miR-10 inhibition. Importantly, arterial and venous gene expression (Online Figure V) was unaffected on miR-10 knockdown compared with control embryos, suggesting that reduced VEGF signaling in MO-miR-10–injected embryos did not alter arterial-venous fate in early vasculogenesis.[8,45]

Reducing FLT1 Levels Rescues miR-10 Knockdown-Induced Defects in Angiogenesis

If FLT1 levels contribute significantly to the defects seen in HUVECs and in zebrafish on miR-10 knockdown, then we hypothesized that reducing FLT1 protein levels could partly

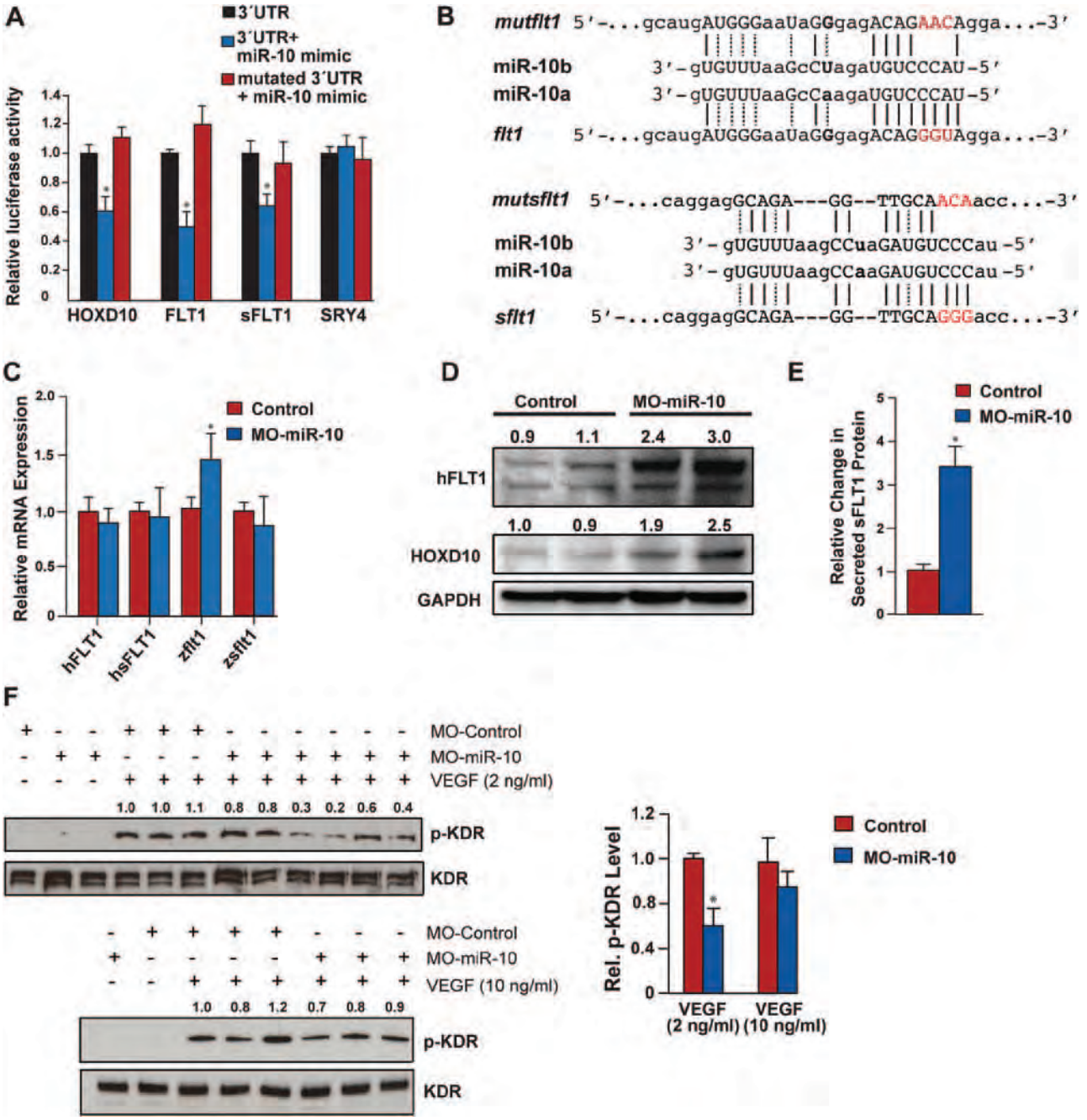

Figure 6. MicroRNA (miR)-10 directly targets fms-related tyrosine kinase 1 (FLT1) and soluble splice variant of FLT1 (sFLT1) to regulate kinase insert domain receptor (KDR) activity. A, Relative luciferase activity of constructs containing 3′ untranslated regions (UTRs) of indicated genes, with or without mutation of putative miR-10 binding site, and with or without miR-10 mimic in COS-7 cells. Homeobox D10 (HOXD10) was used as a positive control. Values displayed as mean±SD, n=3. *P<0.05 compared with 3′ UTR alone. **B**, Target-site complementarity between miR-10 and human FLT1 or sFLT1 3′ UTR, and sequence of mutation in putative miR-10 binding site in FLT1 3′ UTR. **C**, Relative mRNA levels of human (h) and zebrafish (z) flt1/sflt1 in control or miR-10-deficient HUVECs or zebrafish, respectively. *P<0.05 compared with control. **D**, Western blot and densitometric analysis of human FLT1 protein from control or MO-miR-10–transfected endothelial cells 72 hours after transfection. GAPDH was used as a loading control. **E**, Relative change in secreted sFLT1 protein in the supernatant of control or MO-miR-10–transfected HUVECs assessed by ELISA (*P<0.05; n=3). **F**, Immunoblot and analysis of KDR phosphorylation (p-KDR) in HUVECs subjected to low (2 ng/mL) or high (10 ng/mL) concentrations of vascular endothelial growth factor (VEGF) (*P<0.05; n=6).

rescue miR-10 deficiency in endothelial cells. miR-10-deficient HUVECs transfected with a small interfering RNA against human FLT1 responded to VEGF treatment with a noticeable increase in cell number, comparable with that observed in control cells (Figure 7B and Online Figure VII). Immunostaining against the cell proliferation marker phosphohistone H3 revealed that reduction of FLT1 expression in miR-10-deficient HUVECs rescued VEGF-induced proliferation (Figure 7C). In vivo, we coinjected subphenotypic amounts of an established FLT1 MO together with MO-miR-10 and analyzed ISV formation at 36 hpf in *Tg(kdrl:EGFP)s*^{843} embryos.[46] Whereas only 19±5% (n=185) of the embryos injected with

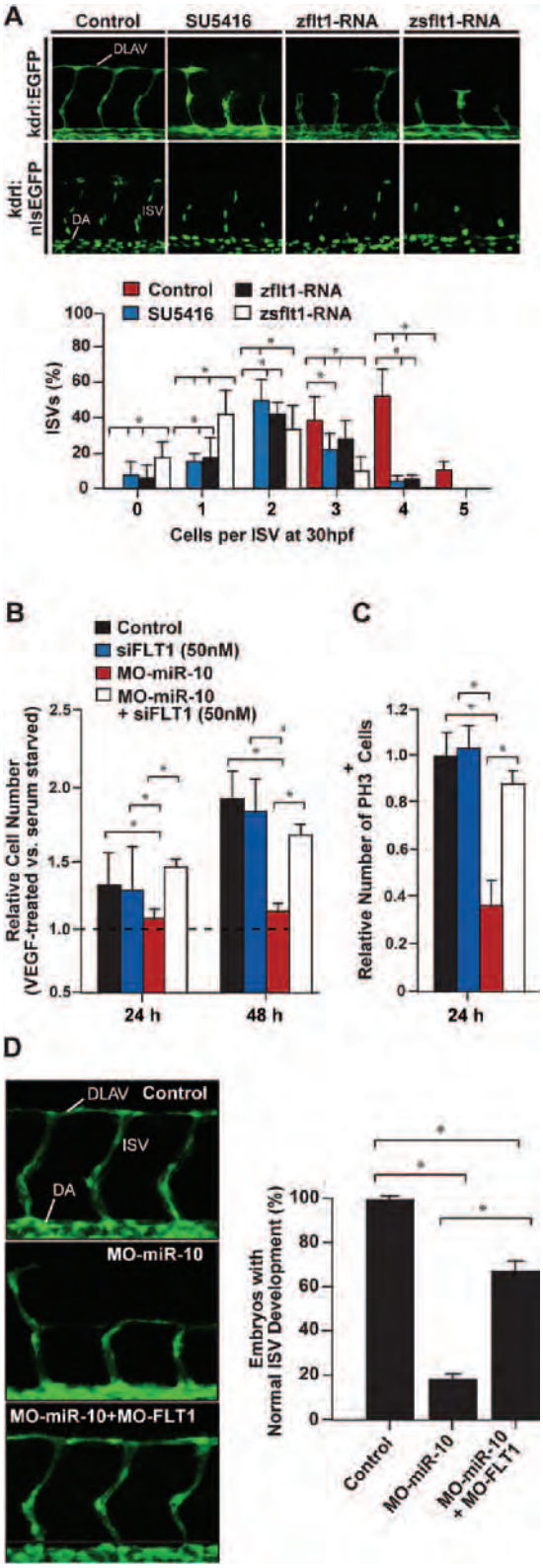

Figure 7. Decreased kinase insert domain receptor (KDR) signaling phenocopies microRNA (miR)-10 deficiency. **A**, Partial inhibition of KDR signaling in zebrafish (30 hours postfertilization [hpf]) by 0.25 μmol/L SU5416 results in intersegmental vessel (ISV) defects similar to miR-10 deficiency. Images are representative high-magnification views. Percent of ISVs with indicated cells/ISV is shown below. Injection of zebrafish fms-related tyrosine kinase 1 (flt1) or soluble splice variant (sflt1) mRNA also resulted in angiogenic defects similar to miR-10–deficiency; ≥200 ISVs from >25 randomly picked larvae per condition were analyzed. B, Relative number of human umbilical venous endothelial cells (HUVECs) in vascular endothelial growth factor (VEGF)-treated vs serum-starved conditions. Control small interfering RNA effects are shown. *P<0.05, n=3. C, Relative number of phosphohistone H3–positive cells after VEGF treatment with siRNA and MO treatment as in B. *P<0.05, n=3. D, High-magnification view of representative ISVs in 30 hpf Tg(kdrl:EGFP)s^{843} zebrafish showing partial rescue of morpholino-microRNA-10 (MO-miR-10)–induced defects in angiogenesis on injection with MO targeting zebrafish flt1 (MO-FLT1). Quantification of ISV defect is shown. *P<0.05, n=150 (control), 185 (MO-miR-10), and 196 (MO-miR-10+MO-FLT1). DA, dorsal aorta; DLAV, dorsal longitudinal anastomotic vessel; zflt1, zebrafish flt1; siFLT1, small interfering RNA against FLT1.

MO-miR-10 alone showed normal ISVs, 63±3% (n=196) of embryos coinjected with FLT1 MO had development of normal ISVs compared with 99±0.5% of all control embryos with normal ISVs (Figure 7D).

Discussion

Here, we provide evidence that miR-10 regulates endothelial cell behavior, and we demonstrate that loss of miR-10 severely affects angiogenesis in vivo. By directly targeting both FLT1 and its soluble splice isoform sFLT1, miR-10 functions to promote KDR-mediated signaling after VEGF exposure and can titrate proangiogenic signaling to fine-tune endothelial cell proliferation, migration, and adhesion.

In zebrafish embryos, we found that loss of miR-10 stalls ISV growth during angiogenesis. ISVs in MO-miR-10–injected embryos had fewer endothelial cells than did controls, indicating reduced proliferation, whereas increasing miR-10 levels produced ISVs with more endothelial cells but without ISV hyperbranching. Pathfinding of dorsally growing ISVs is controlled somewhat independently of VEGF-A. For example, semaphorin-plexinD1 signaling from the adjacent somites acts repulsively to guide endothelial cells during ISV growth.[47] We do not have evidence that increased miR-10 alters these signals, consistent with sprout guidance not being affected in miR-10-overexpressing endothelial cells. However, as described before, we rather found increased endothelial cell number per ISV in miR-10 overexpressing zebrafish larvae as an indicator of increased endothelial cell proliferation and enhanced angiogenic potential.[48] Furthermore, miR-10 deficiency in HUVECs disturbed angiogenic behavior in vitro, whereas increased miR-10 augmented some aspects of angiogenesis. Importantly, the angiogenic potential of miR-10-deficient HUVECs in a matrigel xenograft model was decreased, underscoring the importance of miR-10 in regulating angiogenesis.

We identified FLT1 and its soluble splice variant sFLT1 as direct targets of miR-10 and demonstrated that miR-10 depletion results in elevated FLT1 mRNA levels in zebrafish and increased FLT1 and sFLT1 protein levels in HUVECs. FLT1 is rigidly inserted in the plasma membrane and intrinsically modulates proliferation and migration, whereas sFLT1 functions extracellularly to spatially modulate VEGF availability and to regulate angiogenesis and vessel branching.

Mice lacking FLT1 display endothelial cell overgrowth, blood vessel disorganization, and hyperphosphorylated KDR.[6] Conversely, FLT1 activation causes defects in angiogenesis and endothelial cell proliferation in response to VEGF coincident with reduced KDR phosphorylation, indicating that FLT1 negatively modulates KDR-mediated proangiogenic signaling.[8,49]

In HUVECs, we showed that miR-10 depletion and low-dose VEGF stimulation led to decreased phosphorylation of KDR. This confirms that the upregulation of FLT1 and sFLT1 protein by miR-10 knockdown antagonizes KDR stimulation, most likely because of the higher affinity of both FLT1s for VEGF. Additionally, treatment with the KDR-specific inhibitor SU5416 mimicked the miR-10 knockdown phenotype in zebrafish, suggesting that the observed angiogenesis defects in miR-10-deficient zebrafish is caused by diminished KDR function.

Consistent with previous reports, we demonstrated that overexpression of FLT1 in zebrafish causes reduced ISV sprouting with vessels stalled halfway toward the dorsal root.[50] This phenotype is similar to that of miR-10-depleted embryos, suggesting that FLT1/sFLT1 upregulation on miR-10 knockdown critically contributes to the observed angiogenesis defect. In addition to increased cell numbers per ISV, FLT1 deficiency can result in excessive segmental vessel branching, an effect we did not observe in miR-10 duplex–injected larvae.[50] This discrepancy is likely attributed to the fact that excess miR-10 causes hypomorphic effects by only moderately reducing, rather than completely depleting, FLT1, leaving sufficient protein to influence endothelial cell division without affecting vessel sprouting. Ultimately, the ability to partially rescue the vascular phenotype in miR-10-deficient embryos with concomitant reduction of FLT1 levels suggests that the abnormal angiogenic behavior in endothelial cells lacking miR-10 is, to a great extent, caused by the increase in FLT1 protein.

FLT1 is unlikely to be the only important direct target of miR-10 in endothelial cells, given that FLT1 knockdown incompletely rescues angiogenesis in MO-miR-10–injected zebrafish and incompletely restores proliferation in HUVECs lacking miR-10 at later stages. HOXD10 was described as a very important target of miR-10 in the context of cancer invasion and metastasis.[21] In endothelial cells, HOXD10 overexpression can inhibit angiogenesis,[51] whereas Shen et al[24] recently demonstrated that the known angiogenic or antiangiogenic potential of thrombin or heparin, respectively, is mediated, in part, through regulation of miR-10b and HOXD10. Our data establish FLT1 as a novel target for miR-10 in endothelial cell biology during development and suggest that miR-10 coregulates multiple targets to modulate the angiogenic behavior of vascular endothelial cells. Interestingly, recent reports showed that heparin treatment is accompanied by a strong induction of sFLT1 protein.[52,53]

We found that high-dose VEGF could not rescue the proliferation defect or the reduced angiogenic behavior of HUVECs lacking miR-10, despite the rescue of KDR phosphorylation. In mice, FLT1 depletion can be partially rescued by expressing an FLT1 variant lacking the tyrosine kinase domain.[10] Furthermore, proliferation and branching of vessels derived from FLT1-mutant ESCs can be rescued by soluble sFLT1.[8,10,43] These findings suggest that FLT1 predominantly functions as a sequestering receptor for VEGF, preventing it from binding to KDR, and that the tyrosine kinase domain may be dispensable for FLT1 function during early development. However, others showed that signaling downstream of FLT1 is particularly important for antagonizing KDR-mediated proangiogenic signaling without affecting KDR or mitogen-associated protein kinase phosphorylation.[45,54] Our data favor a dual role of FLT1/sFLT1 in titrating the dose and spatial availability of VEGF, particularly through sFLT1, and a distinct KDR-antagonizing signaling cascade downstream of FLT1. Further studies are needed to dissect the signaling events downstream of FLT1.

With miR-10, we provide evidence of a miRNA that fine-tunes the tightly balanced process of vascular formation by targeting an important growth factor receptor. Our study establishes miR-10 as an important new target to modulate angiogenesis. As FLT1, sFLT1, and miR-10 are expressed in various tissues and are proposed to be involved in the pathogenesis of various diseases, including cancer, studies linking miR-10 levels with FLT1 expression in diseased tissues could provide further mechanistic insights and new opportunities for novel therapeutic approaches.[55–57]

Acknowledgments

The authors thank G. Howard and A.L. Lucido for editorial assistance, B. Taylor for manuscript and figure preparation, members of the Srivastava lab for helpful comments, K. Thorn from the Nikon Imaging Center at University of California, San Francisco, and U. Engel and N. Dross from the Nikon Imaging Center at the University of Heidelberg. Special thanks to L. Juergensen for excellent technical assistance.

Sources of Funding

Dr Hassel was supported by the Deutsche Forschungsgemeinschaft (HA 5819/1-1) and the German Center for Cardiovascular Diseases (DZHK). Dr Ivey was supported by grants from the American Heart Association and the California Institute for Regenerative Medicine (CIRM). D.Y.R. Stainier was supported by grants from the National Institutes of Health (NIH) (HL54737) and the Packard Foundation. Dr Srivastava was supported by grants from National Heart, Lung, and Blood Institute/NIH (U01 HL100406), CIRM, the William Younger Family Foundation, the L.K. Whittier Foundation, and the Roddenberry Foundation. This work was supported by NIH National Institute of General Medical Sciences (T32 GMO7618) to University of California, San Francisco (UCSF), Medical Scientist Training Program (MSTP) and NIH/National Center for Research Resources grant (C06 RR018928) to the Gladstone Institute. Supported by grants from the Deutsche Forschungsgemeinschaft SFB-TR23 "Vascular Differentiation and Remodeling" (project A3 to H.G. Augustin, project Z5 to J. Kroll). H.G. Augustin is supported by an endowed chair from the Aventis Foundation.

Disclosures

Dr Srivastava is on the Scientific Advisory Board of RegeneRx Biopharmaceuticals Inc and iPierian Inc.

References

1. Herbert SP, Stainier DY. Molecular control of endothelial cell behaviour during blood vessel morphogenesis. *Nat Rev Mol Cell Biol*. 2011;12:551–564.
2. Shojaei F. Anti-angiogenesis therapy in cancer: current challenges and future perspectives. *Cancer Lett*. 2012;320:130–137.
3. Ferrara N, Carver-Moore K, Chen H, Dowd M, Lu L, O'Shea KS, Powell-Braxton L, Hillan KJ, Moore MW. Heterozygous embryonic lethality induced by targeted inactivation of the VEGF gene. *Nature*. 1996;380:439–442.
4. Carmeliet P, Ferreira V, Breier G, et al. Abnormal blood vessel development and lethality in embryos lacking a single VEGF allele. *Nature*. 1996;380:435–439.
5. Shalaby F, Rossant J, Yamaguchi TP, Gertsenstein M, Wu XF, Breitman ML, Schuh AC. Failure of blood-island formation and vasculogenesis in Flk-1-deficient mice. *Nature*. 1995;376:62–66.
6. Fong GH, Zhang L, Bryce DM, Peng J. Increased hemangioblast commitment, not vascular disorganization, is the primary defect in flt-1 knock-out mice. *Development*. 1999;126:3015–3025.
7. Fong GH, Rossant J, Gertsenstein M, Breitman ML. Role of the Flt-1 receptor tyrosine kinase in regulating the assembly of vascular endothelium. *Nature*. 1995;376:66–70.
8. Roberts DM, Kearney JB, Johnson JH, Rosenberg MP, Kumar R, Bautch VL. The vascular endothelial growth factor (VEGF) receptor Flt-1 (VEGFR-1) modulates Flk-1 (VEGFR-2) signaling during blood vessel formation. *Am J Pathol*. 2004;164:1531–1535.
9. Seetharam L, Gotoh N, Maru Y, Neufeld G, Yamaguchi S, Shibuya M. A unique signal transduction from FLT tyrosine kinase, a receptor for vascular endothelial growth factor VEGF. *Oncogene*. 1995;10:135–147.
10. Hiratsuka S, Minowa O, Kuno J, Noda T, Shibuya M. Flt-1 lacking the tyrosine kinase domain is sufficient for normal development and angiogenesis in mice. *Proc Natl Acad Sci USA*. 1998;95:9349–9354.
11. Mäkinen T, Jussila L, Veikkola T, Karpanen T, Kettunen MI, Pulkkanen KJ, Kauppinen R, Jackson DG, Kubo H, Nishikawa S, Ylä-Herttuala S, Alitalo K. Inhibition of lymphangiogenesis with resulting lymphedema in transgenic mice expressing soluble VEGF receptor-3. *Nat Med*. 2001;7:199–205.
12. Karkkainen MJ, Ferrell RE, Lawrence EC, Kimak MA, Levinson KL, McTigue MA, Alitalo K, Finegold DN. Missense mutations interfere with VEGFR-3 signalling in primary lymphoedema. *Nat Genet*. 2000;25:153–159.
13. Hogan BM, Herpers R, Witte M, Heloterä H, Alitalo K, Duckers HJ, Schulte-Merker S. Vegfc/Flt4 signalling is suppressed by Dll4 in developing zebrafish intersegmental arteries. *Development*. 2009;136:4001–4009.
14. Covassin LD, Villefranc JA, Kacergis MC, Weinstein BM, Lawson ND. Distinct genetic interactions between multiple Vegf receptors are required for development of different blood vessel types in zebrafish. *Proc Natl Acad Sci USA*. 2006;103:6554–6559.
15. Carmeliet P. Angiogenesis in life, disease and medicine. *Nature*. 2005;438:932–936.
16. Fish JE, Srivastava D. MicroRNAs: opening a new vein in angiogenesis research. *Sci Signal*. 2009;2:pe1.
17. Zhao Y, Samal E, Srivastava D. Serum response factor regulates a muscle-specific microRNA that targets Hand2 during cardiogenesis. *Nature*. 2005;436:214–220.
18. Sabatel C, Malvaux L, Bovy N, Deroanne C, Lambert V, Gonzalez ML, Colige A, Rakic JM, Noël A, Martial JA, Struman I. MicroRNA-21 exhibits antiangiogenic function by targeting RhoB expression in endothelial cells. *PLoS ONE*. 2011;6:e16979.
19. Fish JE, Santoro MM, Morton SU, Yu S, Yeh RF, Wythe JD, Ivey KN, Bruneau BG, Stainier DY, Srivastava D. miR-126 regulates angiogenic signaling and vascular integrity. *Dev Cell*. 2008;15:272–284.
20. Dews M, Homayouni A, Yu D, Murphy D, Sevignani C, Wentzel E, Furth EE, Lee WM, Enders GH, Mendell JT, Thomas-Tikhonenko A. Augmentation of tumor angiogenesis by a Myc-activated microRNA cluster. *Nat Genet*. 2006;38:1060–1065.
21. Wang S, Aurora AB, Johnson BA, Qi X, McAnally J, Hill JA, Richardson JA, Bassel-Duby R, Olson EN. The endothelial-specific microRNA miR-126 governs vascular integrity and angiogenesis. *Dev Cell*. 2008;15:261–271.
22. Ma L, Teruya-Feldstein J, Weinberg RA. Tumour invasion and metastasis initiated by microRNA-10b in breast cancer. *Nature*. 2007;449:682–688.
23. Fang Y, Shi C, Manduchi E, Civelek M, Davies PF. MicroRNA-10a regulation of proinflammatory phenotype in athero-susceptible endothelium in vivo and in vitro. *Proc Natl Acad Sci USA*. 2010;107:13450–13455.
24. Shen X, Fang J, Lv X, Pei Z, Wang Y, Jiang S, Ding K. Heparin impairs angiogenesis through inhibition of microRNA-10b. *J Biol Chem*. 2011;286:26616–26627.
25. Westerfield M. *The zebrafish book. A guide for the laboratory use of zebrafish (danio rerio)*. 3rd ed. Eugene, OR: University of Oregon Press; 1995:385.
26. Jin SW, Herzog W, Santoro MM, et al. A transgene-assisted genetic screen identifies essential regulators of vascular development in vertebrate embryos. *Dev Biol*. 2007;307:29–42.
27. Bussmann J, Bakkers J, Schulte-Merker S. Early endocardial morphogenesis requires Scl/Tal1. *PLoS Genet*. 2007;3:e140.
28. Tanzer A, Amemiya CT, Kim CB, Stadler PF. Evolution of microRNAs located within Hox gene clusters. *J Exp Zool B Mol Dev Evol*. 2005;304:75–85.
29. Lim LP, Glasner ME, Yekta S, Burge CB, Bartel DP. Vertebrate microRNA genes. *Science*. 2003;299:1540.
30. Kloosterman WP, Lagendijk AK, Ketting RF, Moulton JD, Plasterk RH. Targeted inhibition of miRNA maturation with morpholinos reveals a role for miR-375 in pancreatic islet development. *PLoS Biol*. 2007;5:e203.
31. Woltering JM, Durston AJ. MiR-10 represses HoxB1a and HoxB3a in zebrafish. *PLoS ONE*. 2008;3:e1396.
32. Isogai S, Lawson ND, Torrealday S, Horiguchi M, Weinstein BM. Angiogenic network formation in the developing vertebrate trunk. *Development*. 2003;130:5281–5290.
33. Garzon R, Pichiorri F, Palumbo T, Iuliano R, Cimmino A, Aqeilan R, Volinia S, Bhatt D, Alder H, Marcucci G, Calin GA, Liu CG, Bloomfield CD, Andreeff M, Croce CM. MicroRNA fingerprints during human megakaryocytopoiesis. *Proc Natl Acad Sci USA*. 2006;103:5078–5083.
34. Shaw KM, Castranova DA, Pham VN, Kamei M, Kidd KR, Lo BD, Torres-Vasquez J, Ruby A, Weinstein BM. fused-somites-like mutants exhibit defects in trunk vessel patterning. *Dev Dyn*. 2006;235:1753–1760.
35. Schilling TF, Knight RD. Origins of anteroposterior patterning and Hox gene regulation during chordate evolution. *Philos Trans R Soc Lond, B, Biol Sci*. 2001;356:1599–1613.
36. van Eeden FJ, Granato M, Schach U, et al. Mutations affecting somite formation and patterning in the zebrafish, Danio rerio. *Development*. 1996;123:153–164.
37. Laib AM, Bartol A, Alajati A, Korff T, Weber H, Augustin HG. Spheroid-based human endothelial cell microvessel formation in vivo. *Nat Protoc*. 2009;4:1202–1215.
38. Alajati A, Laib AM, Weber H, Boos AM, Bartol A, Ikenberg K, Korff T, Zentgraf H, Obodozie C, Graeser R, Christian S, Finkenzeller G, Stark GB, Héroult M, Augustin HG. Spheroid-based engineering of a human vasculature in mice. *Nat Methods*. 2008;5:439–445.
39. Kearney JB, Ambler CA, Monaco KA, Johnson N, Rapoport RG, Bautch VL. Vascular endothelial growth factor receptor Flt-1 negatively regulates developmental blood vessel formation by modulating endothelial cell division. *Blood*. 2002;99:2397–2407.
40. Lee SH, Schloss DJ, Jarvis L, Krasnow MA, Swain JL. Inhibition of angiogenesis by a mouse sprouty protein. *J Biol Chem*. 2001;276:4128–4133.
41. Roeckl W, Hecht D, Sztajer H, Waltenberger J, Yayon A, Weich HA. Differential binding characteristics and cellular inhibition by soluble VEGF receptors 1 and 2. *Exp Cell Res*. 1998;241:161–170.
42. Kappas NC, Zeng G, Chappell JC, Kearney JB, Hazarika S, Kallianos KG, Patterson C, Annex BH, Bautch VL. The VEGF receptor Flt-1 spatially modulates Flk-1 signaling and blood vessel branching. *J Cell Biol*. 2008;181:847–858.
43. Kearney JB, Kappas NC, Ellerstrom C, DiPaola FW, Bautch VL. The VEGF receptor flt-1 (VEGFR-1) is a positive modulator of vascular sprout formation and branching morphogenesis. *Blood*. 2004;103:4527–4535.
44. Chan J, Bayliss PE, Wood JM, Roberts TM. Dissection of angiogenic signaling in zebrafish using a chemical genetic approach. *Cancer Cell*. 2002;1:257–267.
45. Zeng H, Zhao D, Mukhopadhyay D. Flt-1-mediated down-regulation of endothelial cell proliferation through pertussis toxin-sensitive G proteins, beta gamma subunits, small GTPase CDC42, and partly by Rac-1. *J Biol Chem*. 2002;277:4003–4009.

46. Rottbauer W, Just S, Wessels G, Trano N, Most P, Katus HA, Fishman MC. VEGF-PLCgamma1 pathway controls cardiac contractility in the embryonic heart. *Genes Dev*. 2005;19:1624–1634.
47. Torres-Vázquez J, Gitler AD, Fraser SD, Berk JD, Van N Pham, Fishman MC, Childs S, Epstein JA, Weinstein BM. Semaphorin-plexin signaling guides patterning of the developing vasculature. *Dev Cell*. 2004;7:117–123.
48. Nicoli S, Knyphausen CP, Zhu LJ, Lakshmanan A, Lawson ND. miR-221 is required for endothelial tip cell behaviors during vascular development. *Dev Cell*. 2012;22:418–429.
49. Chappell JC, Taylor SM, Ferrara N, Bautch VL. Local guidance of emerging vessel sprouts requires soluble Flt-1. *Dev Cell*. 2009;17:377–386.
50. Krueger J, Liu D, Scholz K, Zimmer A, Shi Y, Klein C, Siekmann A, Schulte-Merker S, Cudmore M, Ahmed A, le Noble F. Flt1 acts as a negative regulator of tip cell formation and branching morphogenesis in the zebrafish embryo. *Development*. 2011;138:2111–2120.
51. Myers C, Charboneau A, Cheung I, Hanks D, Boudreau N. Sustained expression of homeobox D10 inhibits angiogenesis. *Am J Pathol*. 2002;161:2099–2109.
52. Searle J, Mockel M, Gwosc S, et al. Heparin strongly induces soluble fms-like tyrosine kinase 1 release in vivo and in vitro–brief report. *Arterioscler Thromb Vasc Biol*. 2011;31:2972–2974.
53. Drewlo S, Levytska K, Sobel M, Baczyk D, Lye SJ, Kingdom JC. Heparin promotes soluble VEGF receptor expression in human placental villi to impair endothelial VEGF signaling. *J Thromb Haemost*. 2011;9:2486–2497.
54. Zeng H, Dvorak HF, Mukhopadhyay D. Vascular permeability factor (VPF)/vascular endothelial growth factor (VEGF) peceptor-1 down-modulates VPF/VEGF receptor-2-mediated endothelial cell proliferation, but not migration, through phosphatidylinositol 3-kinase-dependent pathways. *J Biol Chem*. 2001;276:26969–26979.
55. Jongen-Lavrencic M, Sun SM, Dijkstra MK, Valk PJ, Löwenberg B. MicroRNA expression profiling in relation to the genetic heterogeneity of acute myeloid leukemia. *Blood*. 2008;111:5078–5085.
56. Maynard SE, Min JY, Merchan J, Lim KH, Li J, Mondal S, Libermann TA, Morgan JP, Sellke FW, Stillman IE, Epstein FH, Sukhatme VP, Karumanchi SA. Excess placental soluble fms-like tyrosine kinase 1 (sFlt1) may contribute to endothelial dysfunction, hypertension, and proteinuria in preeclampsia. *J Clin Invest*. 2003;111:649–658.
57. Hiratsuka S, Nakamura K, Iwai S, Murakami M, Itoh T, Kijima H, Shipley JM, Senior RM, Shibuya M. MMP9 induction by vascular endothelial growth factor receptor-1 is involved in lung-specific metastasis. *Cancer Cell*. 2002;2:289–300.

Novelty and Significance

What Is Known?

- The formation of new blood vessels is essential for proper embryonic development and progression of diseases, including cancer and retinopathy.
- Angiogenesis relies on a tightly orchestrated network of attractants and repellants controlling the angiogenic potential of endothelial cells, including vascular endothelial growth factors (VEGFs) and their corresponding receptors.
- Posttranscriptional fine-tuning by microRNAs (miRs) can modulate cellular behavior by titrating doses of proteins generated from mRNAs

What New Information Does This Article Contribute?

- Reduction of miR-10 results in severely impaired angiogenic behavior of endothelial cells in vivo in zebrafish and in human endothelial cells in vitro.
- miR-10 directly binds to and regulates the expression of the VEGF sequestering VEGF receptor 1 (fms-related tyrosine kinase 1 [FLT1]) and its soluble splice variant sFLT1.
- A reduction of miR-10 results in an increase in FLT1 protein, which in turn antagonizes proangiogenic signaling mediated by VEGF receptor 2 (kinase insert domain receptor). Thus, miR-10 promotes VEGF-dependent signaling by negatively titrating FLT1.

In the present study, we demonstrate how antiangiogenic FLT1 and proangiogenic kinase insert domain receptor (KDR) signaling is regulated in a miRNA-mediated manner and, thereby, modulate the behavior of endothelial cells during angiogenesis. We show that knockdown of miR-10 in vivo in zebrafish causes severe defects during embryonic angiogenesis with stalled intersegmental vessel growth. Additionally, we demonstrate that reduction of miR-10 function significantly impairs the angiogenic behavior of human endothelial cells. We provide evidence that miR-10 directly regulates the level of the VEGF sequestering receptor FLT1 and its soluble splice variant sFLT1, thereby promoting proangiogenic signaling mediated by KDR. Our findings have potential impact on diseases involving increased or decreased angiogenesis and implicate miR-10 as a novel target for the selective modulation of angiogenesis.

SUPPLEMENTAL MATERIAL

Supplemental Methods

Zebrafish Care and Breeding, Injection Procedures, Inhibitor Treatment, Immunofluorescence and Confocal Microscopy

Care and breeding of zebrafish (*Danio rerio*) was carried out essentially as described.[1] The following strains were used: *Tg(flk1:GFP)*^{s843} and *Tg(flk1:nucGFP; flk1:mCherry)*^{y7} [2, 3] We used two mixtures of morpholino-modified antisense oligonucleotides to knockdown miR-10 activity, targeting dre-pri-miR-10: MO-miR-10 (used in zebrafish and HUVECs) (MO-miR-10b-1: 5′-ACACAAATTCGGTTCTACAGGGTAT-3′; MO-miR-10a: 5′-CACAAATTCGGATCTACAGGGTA-3′; 2–3ng/embryo of each MO was injected) and MO-miR-10* (used in zebrafish only) (MO-miR-10a/c*: 5′-TATTCCCCAAGATACGCATTTGTGA-3′; MO-miR-10b-1*: 5′-TACTCCCCTAGAATCGAATCTGTGA-3′; MO-miR-10b-2*: 5′-TATTCCTGTAGAGACGTATTTGCGA-3′; MO-miR-10d*: 5′-TACTCCCCTAAAACCGAATCTGTGA-3′; 1–2ng/embryo of each MO was injected). Furthermore, the MO against FLT1 in zebrafish that we used was described and validated (MO-FLT1: 5′-CCGAATGATACTCCGTATGTCAC-3′; 1 ng was injected).[4]

For immunofluorescence analysis in zebrafish, the following antibodies were used: MF20 (Developmental Studies Hybridoma Bank; 1:5) and znp1 (Developmental Studies Hybridoma Bank; 1:100).

For the imaging of zebrafish, embryos were embedded in 1% low-melting agarose, and pictures were taken on a Nikon C1si Spectral Confocal (Nikon Imaging Center, UCSF, San Francisco, CA) and on a Nikon A1Rsi 32 channel spectral imaging confocal laser scanning microscope (Nikon Imaging Center, University of Heidelberg, Heidelberg, Germany).

For quantification of ISV growth and ISV cell number, ISVs 5–15 (anterior to posterior) were assayed at indicated stages. 19 hpf *Tg(flk1:GFP)*^{s843} and *Tg(flk1:nucGFP; flk1:mcherry)*^{y7} zebrafish embryos were treated with 0.25 µM U5461 (Sigma-Aldrich) until indicated stages.

Luciferase Assay

Putative 3′UTRs were cloned into pGL3 (Promega) into the 3′UTR of Luciferase using XbaI restrictions sites. Site-directed mutagenesis of 3′UTRs was performed using the QuickChange Lightning Kit (Agilent). Firefly and Renilla luciferase activities were quantified in lysates with the Dual-Luciferase Reporter Assay kit (Promega) on a Victor3 1420 multilabel counter (PerkinElmer), according to the manufacturer's recommendations. Luciferase values were corrected against background and luciferase activity was calculated relative to scrambled control miRNA mimic transfected cells. Renilla activity was used to normalize firefly luciferase values to correct for transfection efficiency.

Transfection/Electroporation of Morpholinos, Mimics and Lentiviral Transduction

For luciferase assays, Cos-7 cells were transfected at 90% confluency with 2 µg of pGL3 (empty, with intact or mutated putative 3′UTR sequence), 300 nM miR-10a/b mimic, 300 nM scrambled control mimic (Dharmacon) and 0.1 µg of Renilla with Lipofectamin 2000 (Invitrogen). At 48 hours post-transfection, cells were lysed and luciferase activity was assayed.

HUVECs were transfected with MO-miR-10 (20 nmol) with the Amaxa Nucleofector Kit for HUVECs (Lonza). For rescue experiments, HUVECs were co-transfected with ON-TARGET*plus* siRNA Smart Pool against human FLT1 (50 nM).

miRZip-lentivector system (System Biosciences) was used to generate miR-10a/b knockdown. miRZip-miR-10a and miRZip-miR-10b was equally used to transduce HUVECs with a total MOI of 40. miRZip-Scramble was used as a control using equal MOI.

Western Blot, ELISA

The following antibodies were used: anti-FLT1 (abcam; 1:500), anti-KDR (Cell Signaling; 1:2000), anti-phospho-KDR (Cell Signaling; 1:1000), anti-GAPDH (Santa Cruz; 1:2000), and anti-HOXD10 (Santa Cruz; 1:200). For phospho-KDR western blots, HUVECs were serum-starved overnight and then treated with 2 or 10 ng/ml as indicated of human recombinant VEGF (BD Biosciences) for 10 min.

For the detection of secreted soluble FLT1 (sFLT1) we used the DuoSet® ELISA Development System against VEGF R1/Flt-1 (R&D Systems) according to the manufacturer's recommendations. Supernatant was derived from control or MO-miR-10 transfected cells cultured for 24h in starving medium with 0.1% FCS.

Cell Culture, Mouse Embryonic Stem Cell Differentiation and FACS

HUVECs and recommended medium were purchased from ScienCell and cultured according to manufacturer's recommendations.

Mouse ES cells were propagated in an undifferentiated form on gelatin-coated cell-culture plastic (Nunc) in GMEM supplemented with 10% FBS, 0.1 mM nonessential amino acids, 2 mM GlutaMAX, 0.1 mM sodium pyruvate (Invitogen), 0.1 mM 2-mercaptoethanol (Sigma-Aldrich), and 1500 U/ml leukemia inhibitory factor (LIF, Millipore). ES cells were passaged every 2–3 days with TrypLE Express (Invitrogen) with daily medium changes. ESC were dissociated to single cells and differentiated as EBs in ultra-low attachment plates (Corning) in GMEM supplemented with penicillin/streptomycin, 2 mM GlutaMAX, 0.1 mM nonessential amino acids (Sigma-Aldrich), and 20% FBS at a final concentration of 100,000 cells/ml. EBs were then replated at day 6 onto gelatin-coated dishes. EBs were digested with accutase and labeled with FITC-conjugated anti-Flk1 (BD Pharmigen 560680) (at 1:50) and APC-conjugated anti-VE-Cad (EBio-17-1441) antibodies in 2% FBS. Cells were resuspended in 0.1% FBS/20 mM Hepes/1 mM EDTA/PBS and sorted on a FACSAria II, and double positive cells were collected.

Capillary Tube Formation Assay, Proliferation, Migration, Adhesion Assay, Spheroid Sprouting Assay and HUVEC Xenografting Assay

The ability of HUVECs to form capillary-like tubes in culture was assayed by adding 8 x10^4 cells to 250 **µ**L of pre-gelled Matrigel (BD Biosciences) in 1 mL of complete medium (ScienCell). The extent of tube formation was subsequently assessed at various time-points after seeding. The kinetics of endothelial cell adhesion were measured by plating cells on uncoated or 0.2% gelatin-coated tissue culture plates and fixing cells after 15, 30 and 60 minutes. The number of DAPI-positive adherent cells was quantified in multiple fields of view. To assay cells survival and proliferation Confluent endothelial cells were serum-starved (0.1% FBS, no growth factors) for 24 or 48 hr in the presence or absence of 2 or 10 ng/mL VEGF as indicated. Cell number was determined by haemocytometer. The percentage of apoptotic cells was quantified after 48 h using an antibody against the apoptosis marker antigen annexin V anti-Annexin V (Abcam; 1:200). Annexin V-positive cells were normalized to the total number of DAPI-positive cells. Proliferating cells were assayed by detecting Histon H3 phosphorylation using anti-phosphohistone H3 (PH3; Cell Signaling; 1:200) antibody. $PH3^+$-cells were normalized to the total number of DAPI-positive cells. Migration of endothelial cells was monitored by generating a 'scratch' in a monolayer of confluent endothelial cells with a P1000 pipet tip and observing the extent of wound closure after 8 or 24 hr. These experiments were performed with complete medium or in basal medium (0.1% FBS, no growth factors) with 2 or 10 ng/mL of VEGF.

Lenti-miRZip-Scramble or Lenti-miRZip-miR-10 transduced HUVECs were used to generate spheroids of defined cell number and used for in-gel sprouting angiogenesis experiments as previously described.[5]

The Matrigel xenografting assay was performed as described.[6, 7] Sections of 0.5µm thickness were produced and stained for human CD34. The stained Matrigel plugs were scanned using a Nikon A1Rsi 32 channel spectral imaging confocal laser scanning microscope. Whole plug area of each plug was assayed for mean vessel density using Fiji software (n=30 from five independent mouse experiments).

Quantitative Reverse Transcription PCR

Quantitative microRNA analysis was performed using TaqMan (Applied Biosystems) and inventoried microRNA assays, according to manufacturer's recommendations. Real-time PCR was performed on diluted samples with miR-16 as an internal control. Gene expression changes were quantified using the delta-delta CT method. Primer sequences are available upon request. To quantify miR-10a and miR-10b expression in mouse embryonic stem cells during differentiation, standard curves were generated using a known amount of miR-10a or miR-10b mimics (Dharmacon).

Statistical Analysis

All experiments were done at least three times in triplicate. Student's t-test or ANOVA was used to determine statistical significance. A p-value smaller then 0.05 was considered as significant.

Supplemental Figures

Supplemental Figure I. The Evolutionary conserved microRNA family miR-10 is encoded within the HOX gene cluster. A, Schematic representation of the genomic localization of miR-10 isoforms within the HOX gene cluster in mammals. miR-10b is predicted to be encoded in hoxd4 overspanning the intron of hoxd3**. B**, Alignment of representative highly conserved miR-10 isoforms in several species. **C**, Alignment of human miR-10a and miR-10b**.** Figure adapted from [8].

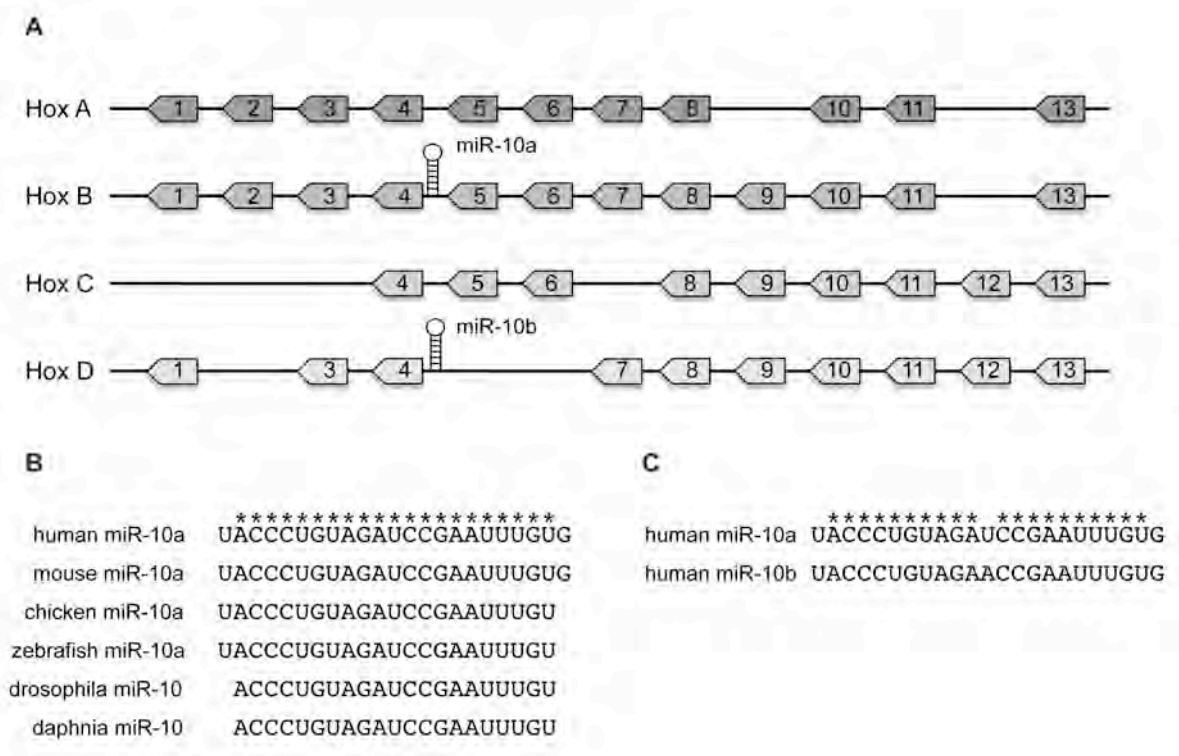

Supplemental Figure II. Knockdown of MO-miR-10* results in abnormal angiogenesis in zebrafish. A, Lateral views of *Tg(flk1:GFP)*^{s843} control injected or MO-miR-10*-injected embryos at 48 hpf. Brightfield images (top) revealed no overall morphological changes upon miR-10 knockdown using MO-miR-10*. Fluorescent images (bottom) showed angiogenesis defects during intersegmental vessel (ISV) sprouting, almost lacking the dorsal longitudinal anastomotic vessel (DLAV), but with normal appearance of the dorsal aorta (DA) and posterior cardinal vein (PCV). For MO-miR-10* injected injection two examples are displayed showing moderate (upper) and severe (lower) characteristics.

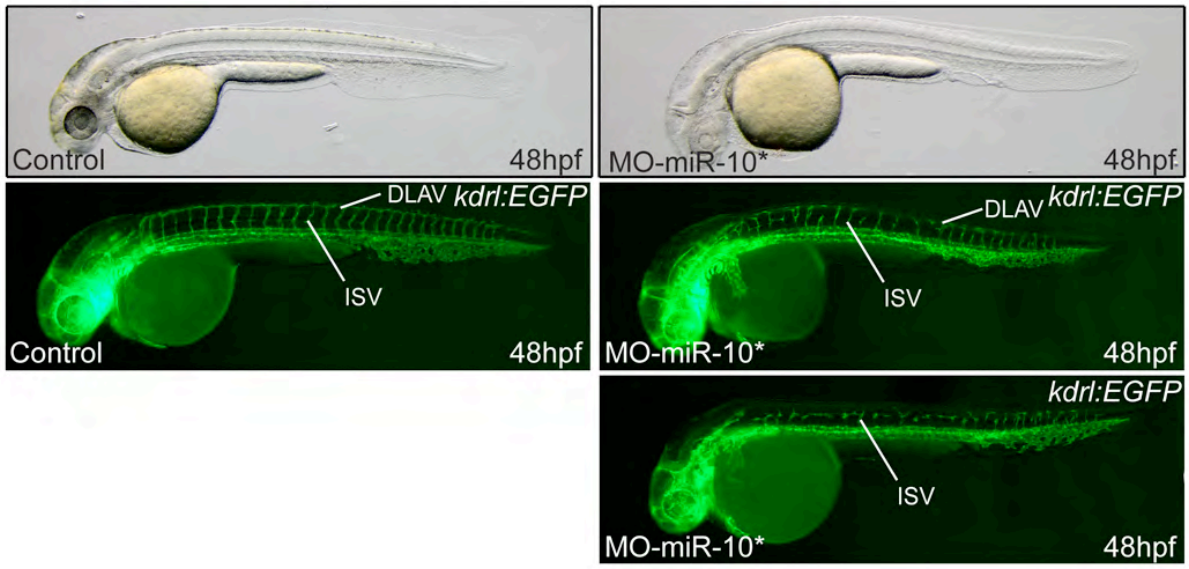

Supplemental Figure III. Lack of miR-10 does not interfere with general morphology and patterning of the somites. A, Lateral view of control and MO-miR-10-injected *Tg(flk1:GFP)*^{s843} zebrafish at 48 hpf immunolabelled with the antibody MF20 (red) to visualize the somites in the trunk. Blood vessels are in green. **B**, Lateral view of *Tg(flk1:GFP)*^{s843} control and MO-miR-10-injected embryos zebrafish embryos at 48 hpf. Motorneurons (red) were immunolabeled with the antibody znp-1, which recognizes synaptotagmin 2. Intersegmental vessels are shown in green. DA, dorsal aorta; DLAV, dorsal longitudinal anastomotic vessel; ISV, intersegmental vessels; MN, motoneurons; NC, notochord; S, somites.

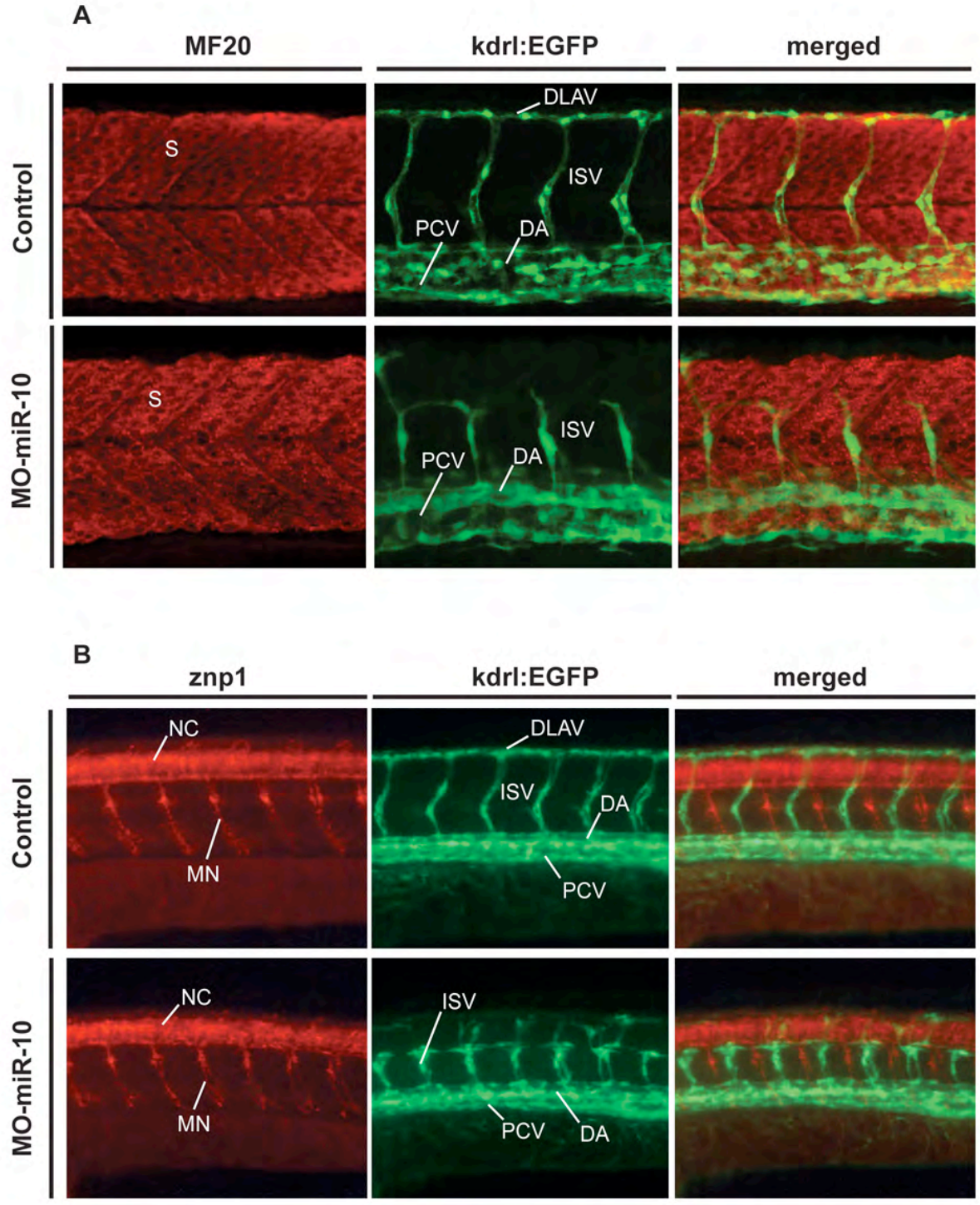

Supplemental Figure IV. miR-10 deficiency affects endothelial cell adhesion. The kinetics of endothelial cell adhesion was assessed by counting the number of attached endothelial cells per view on uncoated (left) and gelatin-coated (right) dishes at indicated times.

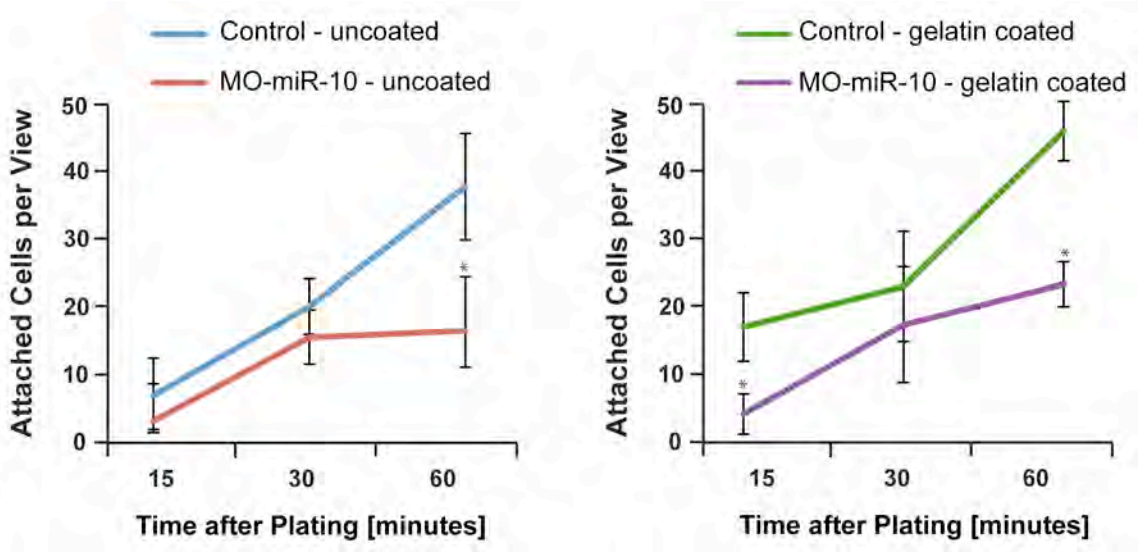

Supplemental Figure V. Knockdown of miR-10 does not affect arterial and venous identity of major trunk vessels. Lateral view of whole-mount in-situ hybridization of control and MO-miR-10-injected zebrafish embryo tails at 24 hpf. The arterial-specific marker ephrinb2a (left) marks the posterior cardinal vein (brackets). The venous-specific marker flt4 (right) is expressed in the dorsal aorta. DA, dorsal aorta; PCV, posterior cardinal vein.

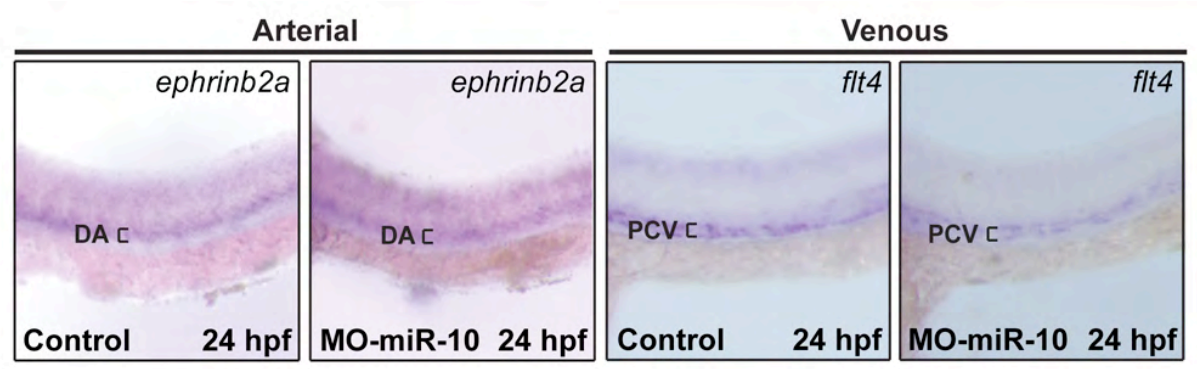

Supplemental Figure VI. Alignment of potential direct miR-10 target sites in predicted human mRNA 3'UTRs. Lines represent complementary base-pairing, and G-U wobble base-pairings are indicated by dotted lines.

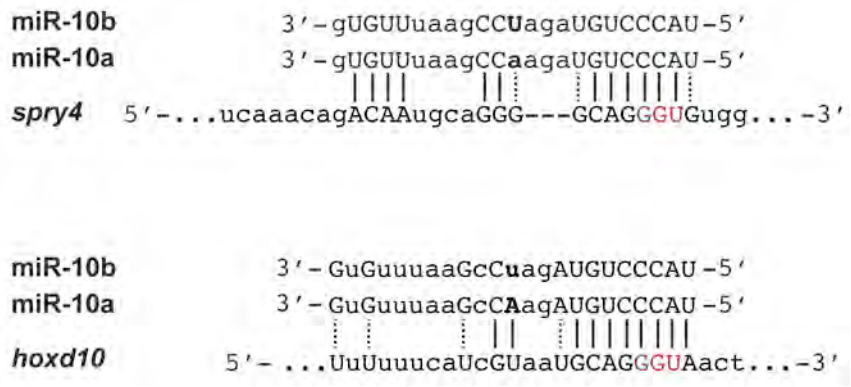

Supplemental Figure VII. Lentiviral-mediated knockdown efficacy of miR-10 in HUVECs. A, Western blot analysis of FLT1 or HOXD10 from miRZip-Scramble (miRZip-Scr; 40MOI) and miRZip-miR-10 (40MOI) transduced HUVECs. GAPDH was used as a loading control. Densitometric analysis of protein levels is indicated above immunoblot. **B,** Representative images of GFP-reporter expression of untransduced, miRZip-Scr or miRZip-miR-10 transduced HUVEC, indicative for infection efficiency. **C,** Western blot analysis of control (left lane) or siFLT-1-transfected HUVECs with the indicated concentrations 48 h post-transfection. Densitometric analysis of FLT1 protein levels is indicated above immunoblot.

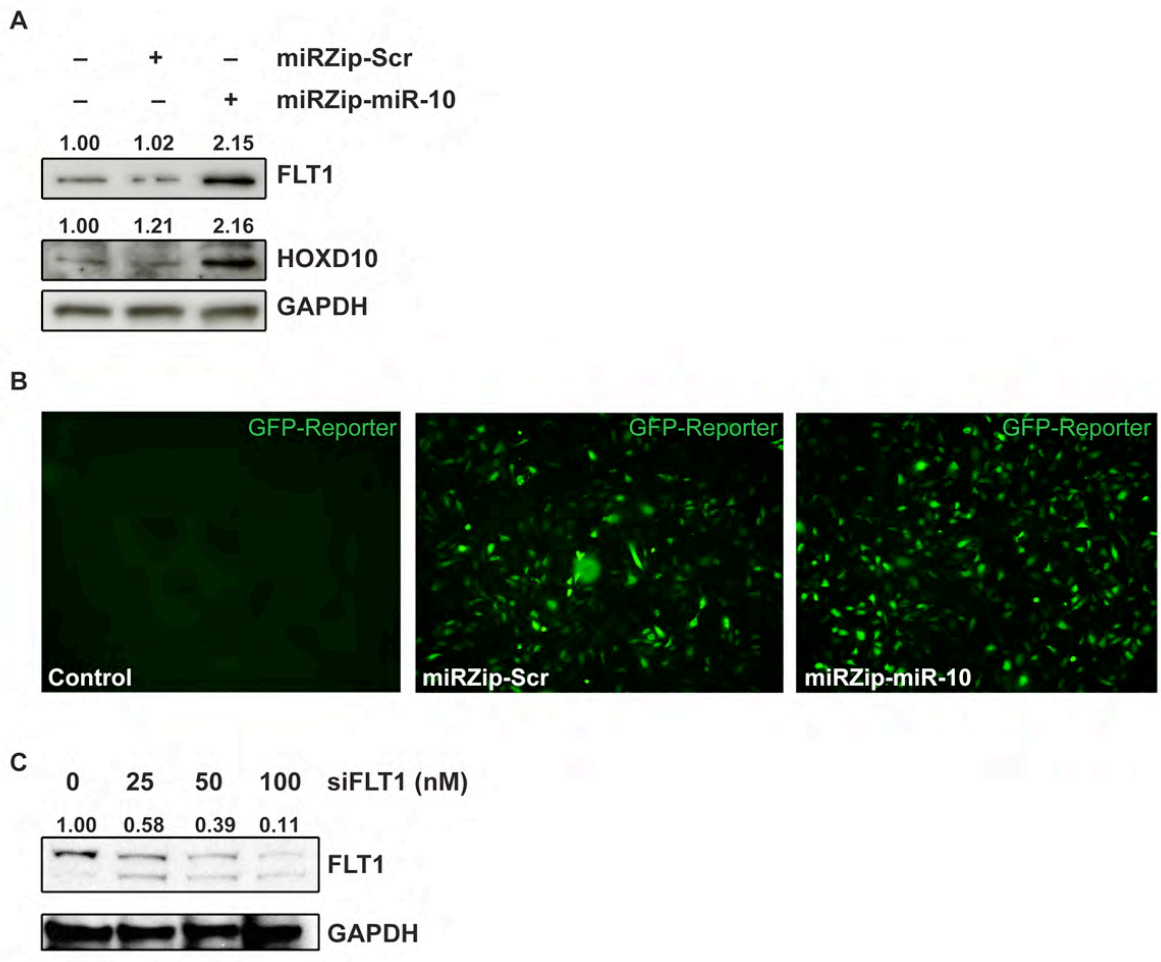

References

1. Westerfield M. The zebrafish book. A guide for the laboratory use of zebrafish (danio rerio), 3rd edition. *Eugene, OR, University of Oregon Press,385 (Book)* 1995.
2. Jin SW, Herzog W, Santoro MM, Mitchell TS, Frantsve J, Jungblut B, Beis D, Scott IC, D'Amico LA, Ober EA, Verkade H, Field HA, Chi NC, Wehman AM, Baier H, Stainier DY. A transgene-assisted genetic screen identifies essential regulators of vascular development in vertebrate embryos. *Dev Biol*. 2007;307:29-42.
3. Bussmann J, Bakkers J, Schulte-Merker S. Early endocardial morphogenesis requires scl/tal1. *PLoS Genet*. 2007;3:e140.
4. Rottbauer W, Just S, Wessels G, Trano N, Most P, Katus HA, Fishman MC. Vegf-plcgamma1 pathway controls cardiac contractility in the embryonic heart. *Genes Dev*. 2005;19:1624-1634.
5. Korff T, Augustin HG. Integration of endothelial cells in multicellular spheroids prevents apoptosis and induces differentiation. *J Cell Biol*. 1998;143:1341-1352.
6. Laib AM, Bartol A, Alajati A, Korff T, Weber H, Augustin HG. Spheroid-based human endothelial cell microvessel formation in vivo. *Nature protocols*. 2009;4:1202-1215.
7. Alajati A, Laib AM, Weber H, Boos AM, Bartol A, Ikenberg K, Korff T, Zentgraf H, Obodozie C, Graeser R, Christian S, Finkenzeller G, Stark GB, Heroult M, Augustin HG. Spheroid-based engineering of a human vasculature in mice. *Nature methods*. 2008;5:439-445.
8. Lund AH. Mir-10 in development and cancer. *Cell Death Differ*. 2010;17:209-214.